



**Institute of Jet Propulsion and
Turbomachinery**
RWTH Aachen University



**RWTHAACHEN
UNIVERSITY**

Student Research Project

Numerical simulation of the flow around the
pectoral fin of a humpback whale

RWTH Aachen University of Technology

Institute of Jet Propulsion and Turbomachinery

**Dr.-Ing. Herwart Hönen
Institute Administration**

**Dipl.-Ing. Jens Andreas
Supervisor**

cand. ing. Carsten Benedikt Wortmann



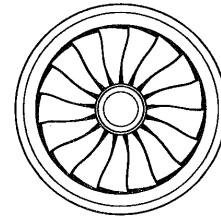
This Page was intentionally left blank.



Subject

Institut für Strahlantriebe und Turboarbeitsmaschinen

Rheinisch-Westfälische
Technische Hochschule Aachen
Institutsleiter: Univ.-Prof. Dr.-Ing. R. Niehuis



Datum: Mai 05

Studienarbeit für Herrn cand.-ing. Carsten Wortmann Matr.-Nr.: 232592

Betreuer: Dipl.-Ing. Jens Andreas, Dipl.-Ing. Kirsten Theobald

Thema:

Numerische Simulation der Umströmung einer Buckelwalflosse

Die Entwicklung von Turbomaschinen hat inzwischen einen so hohen Stand erreicht, dass entscheidende Neuerungen selten geworden sind. Weitere Verbesserungen (z.B. Wirkungsgradsteigerungen) sind jedoch im Hinblick auf die wachsende Umweltproblematik unverzichtbar. Immer öfter werden daher „Techniken“ aus der Natur adaptiert (Bionik), da diese von der Evolution über Jahrtausende optimiert wurden.

Der Buckelwal (megaptera novaeangliae) ist trotz seiner Größe (10-15 m, 25-30 t) ein sehr wendiger und agiler Schwimmer. Ermöglicht wird dies u. a. durch seine im Verhältnis zum Rest des Körpers sehr langen Brustflossen. Dank ihrer ausgefeilten hydrodynamischen „Auslegung“ gestatten diese dem Buckelwal Schwimmmanöver, zu denen andere, ähnlich große Walarten nicht in der Lage sind.

Die auffälligen Tuberkel („Knubbel“) an der Vorderkante der Brustflosse scheinen bei den ausgezeichneten Schwimmeigenschaften dieses Meeressäugers eine wichtige Rolle zu spielen. Zur Klärung der Strömungsphysik soll eine Buckelwalflosse numerisch nachgerechnet werden.

Im Rahmen der Studienarbeit soll daher die Umströmung einer Buckelwalflosse mit Tuberkeln und einer „Referenz-Flosse“ mit glatter Vorderkante numerisch berechnet und verglichen werden.

Im Einzelnen soll die Studienarbeit folgende Arbeiten umfassen:

- Literaturrecherche zur Feststellung der Flossenform und der charakteristischen „Anströmrandbedingungen“
- Einarbeitung in den Netzgenerator ICEM
- Festlegen einer Walflossengeometrie und eines Referenzprofils
- Einarbeitung in den Strömungslöser CFX
- Durchführung der Nachrechnung der Walflosse und des Referenzprofils
- Auswertung der Ergebnisse
- Dokumentation aller Arbeiten

Univ.-Prof. Dr.-Ing. R. Niehuis



Affidavit

I declare that the following report is my work unless otherwise referenced.

Carsten Wortmann
Student ID 232592

January 31st, 2007

Carsten Benedikt Wortmann
Altenhellefelder Str. 28
D-59846 Sundern, Germany

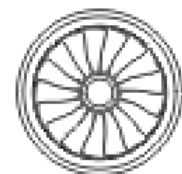
Telephone: +49 177 347 10 52
Facsimile: +49 121 251 385 64 08

Email: Carsten.Wortmann@RWTH-Aachen.de

Institute of Jet Propulsion and Turbomachinery
Templergraben 55
D-52062 Aachen, Germany

Telephone: +49 (241) 80-95500
Facsimile: +49 (241) 80-92-229

Email: web@ist.rwth-aachen.de



**Institute of Jet Propulsion and
Turbomachinery**
RWTH Aachen University

RWTHAACHEN



Executive Summary

The core of this thesis is to simulate the flow around a humpback whale's pectoral fin numerically using computational fluid dynamics (CFD). A clean pectoral fin with a smooth leading edge is taken as a reference for comparing the outcomes of this simulation. This subchapter will provide a brief summarization on how this objective is accomplished, what recommendations can be concluded from this thesis and what steps had to be taken prior to this numerical simulation.

Among whales, the humpback whale attracts attention due to its extraordinary long and flexible flippers. These flippers are suspected to be the reason for an extreme maneuverability despite its body length and weight. As an important difference to other species' flippers, tubercles ("knobs") are attached to the fin's leading edge. Publications suggest that because of those tubercles under some circumstances drag decreases up to 30% while lift and angle of attack for stalling increases significantly [14]. In terms of biomimicry it has to be examined if this effect can be used for improving airfoils (e.g. engine blades, grids or wings) as well.

Consequently, some background data about the humpback whale is found through literature research. Information about movements and dive patterns is gathered. Accordingly, papers considering the flipper are analyzed to identify, digitalize and import a default flipper into a CFD program.

For identification, numerous photographs of individual humpback whales are merged and a two-dimensional top view of a typical pectoral fin is drawn by hand. It is subsequently scanned and converted to a bitmap file for digitalization. Developing a three-dimensional flipper the thickness has to be considered. Scientific papers state that maximum thickness can be found from 49% to 19% in the mid-span. However, the maximum thickness ratio varies from 0.20 to 0.28, averaging at 0.20-0.23 [9]. This would lead to a NACA 0020 airfoil. However, comparison with photographs of living whales in the task relevant swimming maneuver suggested the use of a thinner profile. Thus, thickness and shape of the flipper are calculated according to the NACA 0012 airfoil. Two versions of the pectoral fin, one with and one without tubercles are saved as an IGES file and imported into the meshing tool Ansys Icem CFD.

As a last step prior to flow simulation, a numerical mesh has to be created. In this case, a hexahedron grid is chosen as this type is supposed to be the best for numerical analysis. The strategy for creating a suitable mesh is to use blocking around the fin, an O-grid for better resolution of boundary effects and compressing the grid at tip and shoulder for better resolution.

However, exporting the mesh to the CFX solver revealed several inconsistencies, holes and breaks on the flipper surface. This is found due to an inaccurate mesh and also not ideal meshing type. Therefore, inconsistent surfaces and limits in the creation possibilities suggest using a tetrahedral mesh instead. This meshing type can be created using a lot more parameters and automatisms. In addition, it is better suited for complex geometries.

In following reports based on this thesis, improvements in fluid dynamics still have to be validated through an alternative approach to this subject. In addition, besides these observations, the exact explanations of the mechanisms leading to this effect have to be analyzed. However, if this is successful, it needs to be considered if improvements in this way on existing aerodynamic applications are reasonable and cost-efficient.



Acknowledgements

I would like to give sincere thanks to all who aided me in any imaginable way during my work at the RWTH Institute of Jet Propulsion and Turbomachinery in Aachen.

For the assistance and initial training and supervision I would like to say thanks to Dipl.-Ing. Jens Andreas, former scientific assistant at the IST, Institute of Jet Propulsion and Turbomachinery in Aachen and Prof. Dr.-Ing. R. Niehuis, former head of this institute. I would like to thank them also for making this project possible. For their help during the first stages of this work, I would like to articulate acknowledgements to Dr. Frank E. Fish, Department of Biology, West Chester University, and Dr. Meike Scheidat, Research- and Technology Centre Westcoast, Christian-Albrechts University Kiel. Proof-reading was done by cand. Ing. Alexander Salert. Additionally, for their continuous support and encouragement, I would like to express my gratitude to my family and friends.

Without any of the mentioned above my work on this topic would not have been that successful.

Dr.-Ing. Herwart Hönen

Institute of Jet Propulsion and Turbomachinery
Templergraben 55
D-52062 Aachen
Germany



**Institute of Jet Propulsion and
Turbomachinery**
RWTH Aachen University

Dipl.-Ing. Jens Andreas

Institute of Jet Propulsion and Turbomachinery
Templergraben 55
D-52062 Aachen
Germany



Index

Contents

Subject	3
Affidavit	4
Executive Summary	5
Acknowledgements	6
Index	7
Contents	7
List of Figures	9
List of Tables	11
List of Abbreviations	12
1 Introduction	13
1.1 Preamble	13
1.2 Biomimicry	13
1.3 Task	14
1.4 Thesis Structure	16
2 The Humpback Whale	17
2.1 Scientific Classification	17
2.2 Typical Characteristics	18
2.2.1 Habitat and Behavior.....	18
2.2.2 Whale Song.....	21
2.2.3 Parasites.....	22
2.3 Research Related Details	23
2.3.1 The Flipper.....	23
2.3.2 Hydrodynamic Flow.....	26
3 State of Affairs	29
3.1 Current Innovations based on Flow Control	29
3.1.1 High Lift Devices.....	30
3.1.1.1 Leading edge.....	30
3.1.1.1.1 Variable camber leading edge.....	31
3.1.1.1.2 Simple and folding bull-nose Krueger flap.....	31
3.1.1.1.3 Slats.....	32
3.1.1.2 Trailing edge.....	32
3.1.1.2.1 Flaps.....	32
3.1.2 Other boundary layer control devices.....	32
3.1.2.1 Passive vortex generators.....	33
3.1.2.2 Air-jet vortex generators.....	34
3.2 Previous Research on Pectoral Fins	36



4	<i>Digitalization of a Humpback Whale’s Flipper</i>	38
4.1	Preliminary Considerations and Modeling	38
4.2	Drawing the planform	39
4.3	Reading the Bitmap	40
4.3.1	The “kkonvert.c” BMP-to-Coordinate Converter	41
4.4	The Flipper’s System of Coordinates	42
4.5	Data Processing in LabView, TecPlot and Excel	42
4.6	Generation of a Third Dimension	44
4.6.1	Finding the NACA airfoil	44
4.6.2	Scaling the NACA Wing Design	45
4.6.3	Calculation of Z-Values	45
4.7	Troubleshooting ProE	47
4.8	Generation of Digitalized Pectoral Flipper with Tubercles	49
4.9	Import into ProE Wildfire 2.0	53
4.10	Export as IGES File	53
4.11	Simplifications and Troubleshootings	55
5	<i>The Mesh</i>	56
5.1	The Hexa Mesh in Theory	57
5.1.1	O-Grid	57
5.1.2	Edge-Meshing Parameters	58
5.1.3	Time Saving Methods	58
5.1.4	Hexa Database	59
5.1.5	Unstructured and Structured Mesh Output	59
5.2	Meshing the Pectoral Fin	60
5.2.1	Blocking	60
5.2.2	Assigning Material	61
5.2.3	Creating the O-Grid	62
5.2.4	Mesh Parameters	63
5.2.5	Mesh around Pectoral Fin without Tubercles	63
5.2.6	Export to CFX	65
5.3	Troubleshootings and Problems	67
6	<i>Conclusion and Recommendation</i>	68
7	<i>References</i>	69
8	<i>Appendix</i>	71
8.1	The “kkonvert.c” BMP-to-Coordinate Converter	71
8.1.1	Program Code	71
8.2	CD Index	76
8.3	Additional Tables	77
8.4	About the Author	81



List of Figures

Figure 1-1: Pectoral Fin [21]	13
Figure 1-2: Gliding Vulture [10]	14
Figure 1-3: Bionic Sailing Wing [16]	14
Figure 1-4: Flaps during Landing Approach	15
Figure 1-5: Slats and Flaps, A320-300 [8].....	15
Figure 1-6: Megaptera Novaeangliae [18].....	15
Figure 2-1: Megaptera Novaeangliae [26].....	17
Figure 2-2: Humpback Whale Range [8].....	18
Figure 2-3: Breeding and Feeding Areas [22]	18
Figure 2-4: Jumping Humpback Whale [6].....	19
Figure 2-5: Whale accompanied by Calve [6]	19
Figure 2-6: Echo Sounder Tracings.....	20
Figure 2-7: Distribution of foraging dives	21
Figure 2-8: Distribution of foraging bouts.....	21
Figure 2-9: Idealized dolphin head showing the regions involved in sound production. [8]	22
Figure 2-10: Humpback Whale song spectrogram (Listen to Song on CD) [8]	22
Figure 2-11: Whale lice, 5-25 mm length [8].....	22
Figure 2-12: Barnacles [8].....	22
Figure 2-13: Flipper planform with representative cross-sections [9].....	24
Figure 2-14: Humpback whales in Southeast Alaska [1]	24
Figure 2-15: Distance between tubercles [9]	25
Figure 2-16: Position of max. thickness [9].....	25
Figure 2-17: Skeleton Megaptera Novaeangliae [28].....	25
Figure 2-18: Humpback whale from side, top and head-on view [19]	27
Figure 2-19: Reynolds Number for Boundary Conditions [8].....	28
Figure 3-1: Optimization process over time.....	29
Figure 3-2: Commercial airplane taking off using high lift devices [12]	30
Figure 3-3: Three different leading edge devices [2]	30
Figure 3-4: Variable camber leading edge [8]	31
Figure 3-5: Krueger flap of a Boeing 737-300 partially extended [7].....	31
Figure 3-6: Four different types of flaps [8]	32
Figure 3-7: Vortex generators installed on upper wing surface [Maule Air Inc.]	33
Figure 3-8: Different vortex generator configurations	35
Figure 3-9: Boundary Layer Changes through Vortex Generators [17].....	35
Figure 3-10: Simulation of Flow without Tubercles [23].....	36
Figure 3-11: Simulation of Flow with Tubercles [23].....	36
Figure 3-12: Streamlines outside Boundary Layer on Tubercle [23].....	36
Figure 3-13: Wind Tunnel Models of Pectoral Fins w/ and w/o Tubercles [14]	37



Figure 4-1: Sketch of humpback whale’s pectoral fin without tubercles..... 39

Figure 4-2: Sketch of humpback whale’s pectoral fin with tubercles 39

Figure 4-3: Colored out flipper sketch 40

Figure 4-4: Desired pixel course, no doubles, no gaps 40

Figure 4-5: Pixel course, double pixel 41

Figure 4-6: Pixel course, gap 41

Figure 4-7: Coordinates from flipper drawing, without tubercles 41

Figure 4-8: Pectoral Fin System of Coordinates, X-Y Layer 42

Figure 4-9: Airfoil System of Coordinates..... 42

Figure 4-10: Excel Output for Pectoral Fin without Tubercles..... 44

Figure 4-11: Excel Output for Pectoral Fin with Tubercles 44

Figure 4-12: Cuts and Sections within Pectoral Fin 45

Figure 4-13: TecPlot Fin Printout 46

Figure 4-14: Error in Pectoral Fin Surface, ISO View 47

Figure 4-15: Error in Pectoral Fin, Head-On View 47

Figure 4-16: Screenshot of Pectoral Fin without Tubercles..... 48

Figure 4-17: Confrontation Chord Length w/ and w/o Tubercles 50

Figure 4-18: Pectoral Fin Pattern and Chord Length including Tubercles 51

Figure 4-19: Sequence of Coordinate Data around Fin Pattern 51

Figure 4-20: Leading and Trailing Edge of Pectoral Fin with Tubercles..... 52

Figure 4-21: Example for axis situation and coordinate value. 53

Figure 4-22: Screenshot Pectoral Fin with Tubercles..... 54

Figure 5-1: Hybrid Grid [4] 56

Figure 5-2: Tetrahedron Grid [4]..... 56

Figure 5-3: 2D Hexa Grid [24] 56

Figure 5-4: 3D Auto Hexa Grid around Car [4] 56

Figure 5-5: Initial block..... 58

Figure 5-6: Block with O-Grid 58

Figure 5-7: Block with O-Grid and including a face 58

Figure 5-8: Blocking Strategy around wing 60

Figure 5-9: Creating Parts Interface for defining Material 62

Figure 5-10: Surface Mesh Size Dialogue Screen 63

Figure 5-11: Mesh around Pectoral Fin 64

Figure 5-12: CFX Imported Mesh..... 66

Figure 5-13: Zoom on meshed Flipper in CFX 66

Figure 6-1: Flowchart of further recommendations on this topic..... 68



List of Tables

Table 4-1: Set of Equations for NACA scaling 45
Table 4-2: Set of Equations for chord scaling 46
Table 4-3: TecPlot Database Abstract 46
Table 8-1: List of Coordinates for Pectoral Fin without Tubercles..... 77
Table 8-2: List of Coordinates for Pectoral Fin with Tubercles 78
Table 8-3: Airfoil Cuts for Pectoral Fin with Tubercles..... 79
Table 8-4: Translations..... 80



List of Abbreviations

ASCII	American Standard Code for Information Interchange, character encoding based on the English alphabet
Autohexa	Automatic Hexa Mesh Generator within ICEM
CAD	Computer Aided Design
CFD	Computational Fluid Dynamics
CFX	Solver for Fluid Dynamics Simulations, connected to CFD
C_{Lmax}	Maximum Lift
DOS	Disk Operating System, dominated the IBM compatible market
I	Number of NACA airfoil points
IBM	International Business Machines, personal computer competing with Commodore and Apple
ICEM	Company developing CFD Software, lately bought by ANSYS
IGES	International Graphics Exchange Standard
J	Cuts in the direction of X
L	Characteristic length (equal to diameter (2r) if a cross-section is circular)
l/d	Lift to drag ratio
L01, L	Overall length of flipper
NACA	National Advisory Committee for Aeronautics
NURBS	Non-uniform, rational B-spline, mathematical model commonly used in computer graphics for generating and representing curves and surfaces
ProE	Parametric feature-based three-dimensional Solid modeling CAD software created by Parametric Technology Corporation (PTC)
pts	File type containing flipper's coordinates (points) in ASCII format
Re	Reynolds Number
s	Scale factor
T01	Profile length
TXT	DOS ASCII text file
UltraEdit	Text editor for Microsoft Windows created by IDM Computer Solutions
US	United States
VC	Variable camber (Krueger flaps)
vi	Virtual Instrument (LabView)
v_s	Mean fluid velocity
w/	Common Abbreviation: with
w/o	Common Abbreviation: without
x, y, z	Coordinates for fin, NACA profile or scaled image
X1	Leading edge X coordinates
X2	Trailing edge X coordinates
XLS	File type for Microsoft Excel
α	Angle of Attack
α_{Stall}	Angle of Attack for Stalling Behavior
μ	(Absolute) dynamic fluid viscosity
ν	Cinematic fluid viscosity: $\nu = \mu / \rho$
ρ	Fluid density

1 Introduction

1.1 Preamble

Humpback whales (*megaptera novaeangliae*) impress by astonishing maneuverability considering their size (13 meters, 30 metric tons). Compared to other marine mammals the *megaptera novaeangliae* possesses unusually long pectoral fins ("flippers"). From the aerodynamic point of view the speculation arises whether these pectoral fins play a decisive part in the whale's maneuverability. Apart from their length the flippers are marked by another peculiar feature: The tubercles on their leading edge, figure 1-1. Understanding the flow physics involved may yield interesting possibilities for the improvement of aerodynamic devices.



Figure 1-1: Pectoral Fin [21]

Biologists assume that these tubercles might play an important role regarding this outstanding agility. Using this feature for certain airfoils might be the key for a further evolutionary step.

1.2 Biomimicry

Evolution of aerodynamic applications reached such a high standard, that decisive innovations became very rare. In an attempt to reduce the environmental impact of today's technology e.g. by optimizing existing concepts, engineers labor to adapt biological concepts to their work.

The application of methods found in the environment to the design of engineering systems is called "bionics". As a short form for "biomechanics", this word is set together from two words, biology (originated in the Greek word "βίος", pronounced "vios" and meaning "life") and electronics [8]. As this way of discovering technical improvements has less to do with just electronics, but with every other technical field of investigation as well, an even better translation of the German "Bionik" can be found: "biomimicry". Biomimicry is composed of the words bios and mimicry and can be understood as a conscious strategy by designers to observe and learn principles of design from nature.



As an example for biomimicry, a glider's wing tip was designed according to the raven-vulture shown in figure 1-2. While observing possible prey, the vulture braces the wing-tip feathers. Through fanning out these feathers, these vultures can cut wing-tip-vortices into small turbulences, which decrease energy loss.

This effect has been used for a glider's wing. Although now specific research shows that this type of wing tip is not necessary at big spans, figure 1-3 gives an example of biomimicry in this matter.



Figure 1-2: Gliding Vulture [10]



Figure 1-3: Bionic Sailing Wing [16]

Aircrafts in general can be seen as another example for biomimicry. Looking at early aircrafts, the use of this method is obvious, as they resemble avian animals. But this example is also quotable to show that biomimicry can also be misleading, for motorized flying was only possible after separating propulsion from lift. Thus, it can be helpful to look at nature, but in some cases, maybe even in this case, it might be necessary to even think beyond natural evolution.

1.3 Task

The aim of this thesis is to create a three-dimensional numerical model of a humpback's flipper and to mesh it to allow an analysis using computational fluid dynamics (CFD). This task can be divided into the following steps.

First, literature research has to be done. During cruise speed, the clean wing is considered to be the optimum configuration. However, for take-off and landing high lift systems are required. An example for these devices can be seen in figure 1-4 and figure 1-5. As the humpback whale's pectoral fins will enhance flow control in these flight situations, current innovations already established on aircrafts need to be reviewed for comparison. This is necessary to have a reference for the efficiency of tubercle attached wings in correspondence to clean wings.

**Figure 1-4: Flaps during Landing Approach****Figure 1-5: Slats and Flaps, A320-300 [8]**

Also, more information has to be gathered about the humpback whale in general, e.g. its habitat, breeding and feeding area, foraging habits and maneuverability. Figure 1-6 shows the humpback whale in an upward movement, extremely bending its pectoral fin.

**Figure 1-6: Megaptera Novaeangliae [18]**

Subsequently, the pectoral fin has to be analyzed in further detail. For identification and digitalization data about thickness, span, and amount of tubercles needs to be collected. Finally in literature research, details about the characteristic flow situation, e.g. velocity, depth and angle of attack, must be found out to set up the boundary conditions of the planned CFD-calculations.

Data collected during literature research shall be used for creating a typical geometry and a reference profile of the humpback whale's flipper. These two versions need to be digitalized and provided as an importable file for Ansys ICEM CFD.

After initial training on Ansys ICEM CFD and CFX, a numerical mesh around both versions of the flipper has to be created within CFD, and exported to the solver CFX. The flow around these flippers has to be simulated and compared to each other, to document advantages and disadvantages of both types. All results need to be stated.

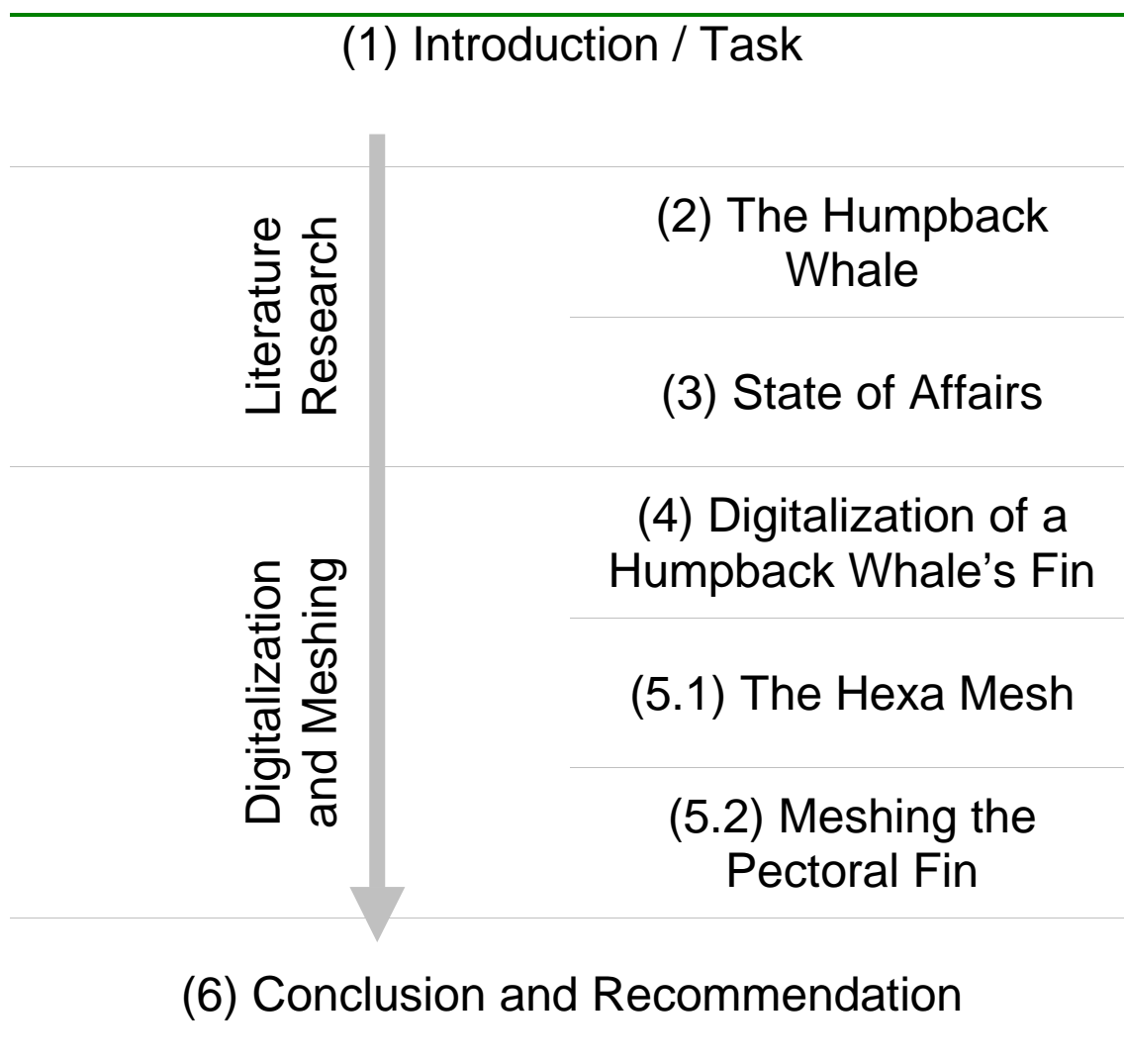


1.4 Thesis Structure

This thesis is divided into two major parts. The first part will deal with literature research to provide general knowledge about the topic. The humpback whale is described in detail, and especially the pectoral fin will be pictured. In the next chapter, research already done on this topic will be described.

The next two chapters will deal with the digitalization and meshing of the flipper. Finally, the last chapter will give a conclusion and recommendation for further research on this topic.

This divisiveness is displayed in the thesis structure hereafter.



2 The Humpback Whale

This chapter provides a classification of the humpback whale and gives background information of its natural surroundings. In addition, typical characteristics and details regarding the pectoral fins are described.

2.1 Scientific Classification

The scientific name for a humpback whale, *Megaptera novaeangliae*, is taken from Greek and Latin. Megaptera stands for the Greek “megas” and “pteron”, meaning “Great Wing”, grabbing the one but most flamboyant characteristic, the long pectoral fins. Novaeangliae is Latin for “New England”, where this whale was first observed.

The humpback whale has a barrel-shaped body reducing its diameter from head to fluke. The head itself is flattened and usually very tuberculous. The very long, aliform flipper makes up one third of the over all body length (figure 2-1).

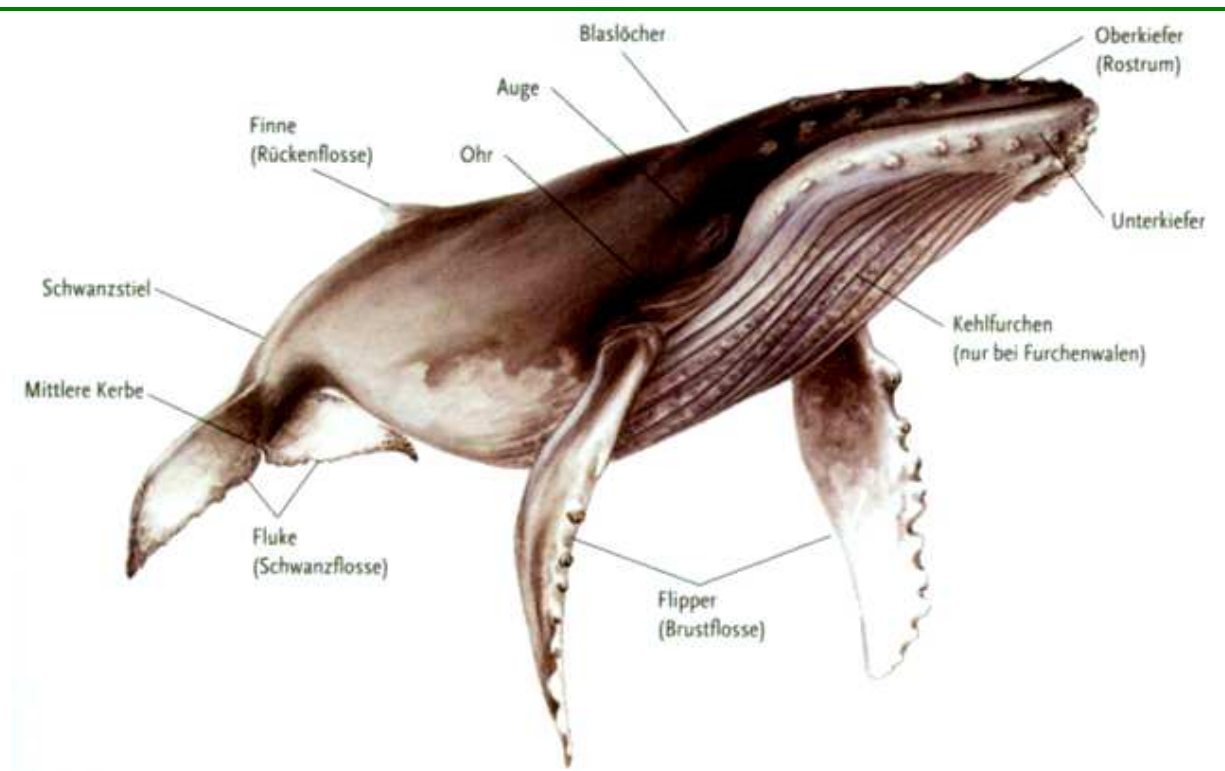


Figure 2-1: *Megaptera Novaeangliae* [26]

A translation of the German vocabulary in this figure can be found in table 8-4.



In scientific classification, the humpback whale belongs to the kingdom *animalia* (lt. animals). Other kingdoms are known as *plantae* (lt. plants), *fungi* (lt. mushrooms) and *viridae* (lt. viruses). Within the kingdom, it belongs to the phylum *chordata* (lt. chordates), in which mainly oceanic animals, around 60,000 species, are combined. Inside the phylum, it can be classified as *mammalia* (lt. mammals), such as humans. The corresponding subclass is called *eutheria*, a group of organisms containing the placental mammals. The humpback whale belongs to the order *cetacea* (lt. whales), which is composed from Greek *ketos* meaning “monster of the sea” and the Latin *cetus* meaning “great animal of the ocean”. This order is divided into two suborders, *odontoceti* (lt. toothed whales) and *mysticeti* (lt. baleen whales). Within the suborder *mysticeti*, the humpback whale belongs to the family *balaenoptiidae* (lt. rorquals). Other rorquals are the mink whale, the grey whale and the blue whale.

2.2 Typical Characteristics

The humpback whales upper body's color is black sometimes fading into blue, the bottom side can be white, black or brindled. An adult humpback whale ranges between 12-16 m long and can weigh up to 36,000 kg [8].

2.2.1 Habitat and Behavior

The humpback whale lives in oceans and seas all over the world (figure 2-2). In fact the area where the humpback whale can be observed permanently is up to 40,000 km² large. As breeding and feeding areas are far apart from each other, the humpback whale has to manage large traveling distances (figure 2-3). Annual voyages of approximately 25,000 km are common [8].

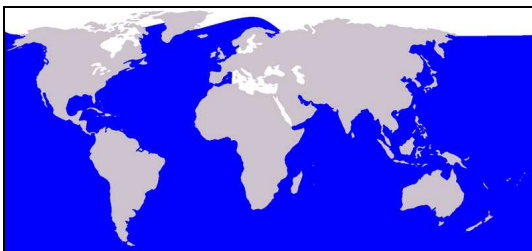


Figure 2-2: Humpback Whale Range [8]

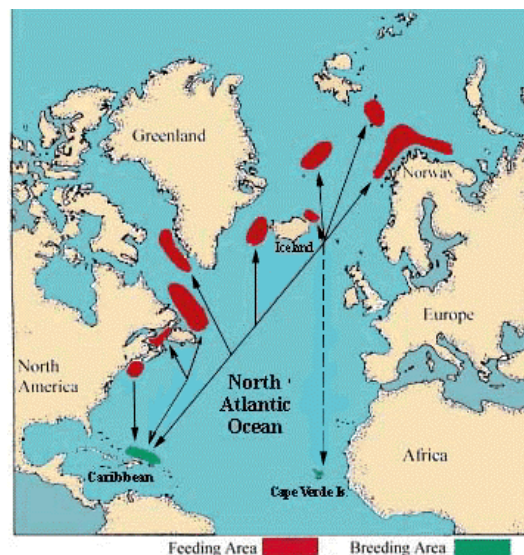


Figure 2-3: Breeding and Feeding Areas [22]



Sometimes, males jump out of the water high showing their tail fin while diving into the water again, as in figure 2-4. It is not clear whether this is to impress females or loose parasites (chapter 2.2.3).

Breeding can only take place in warm areas. On the other side, prey (e.g. krill) is more prosperous in northern areas. Calves would suffer death from cold as they are born without the protecting grease padding [25]. Figure 2-5 shows a cow accompanied by her calve. Humpback whales can be together with their offspring for more than four years.



Figure 2-4: Jumping Humpback Whale [6]



Figure 2-5: Whale accompanied by Calve [6]

Considering foraging dive patterns of humpback whales in southeast Alaska [5], it is not known that dive habits changed in the last years, so this report on humpback whale's dive patterns can be taken as representative.

During summer of 1979 to 1984, diving, ventilation and surface behavior was recorded. All observations were taken using an echo sounder with good observation within the top 260 m of the water column. The water column was partitioned into 20 m depth intervals between 0 and 260 m.

As it is shown in figure 2-6, surface feeding depth is from 0-20 m. While releasing the camera, whales were found from 80-95 m swimming close to a layer of dense krill reaching down to 120 m.

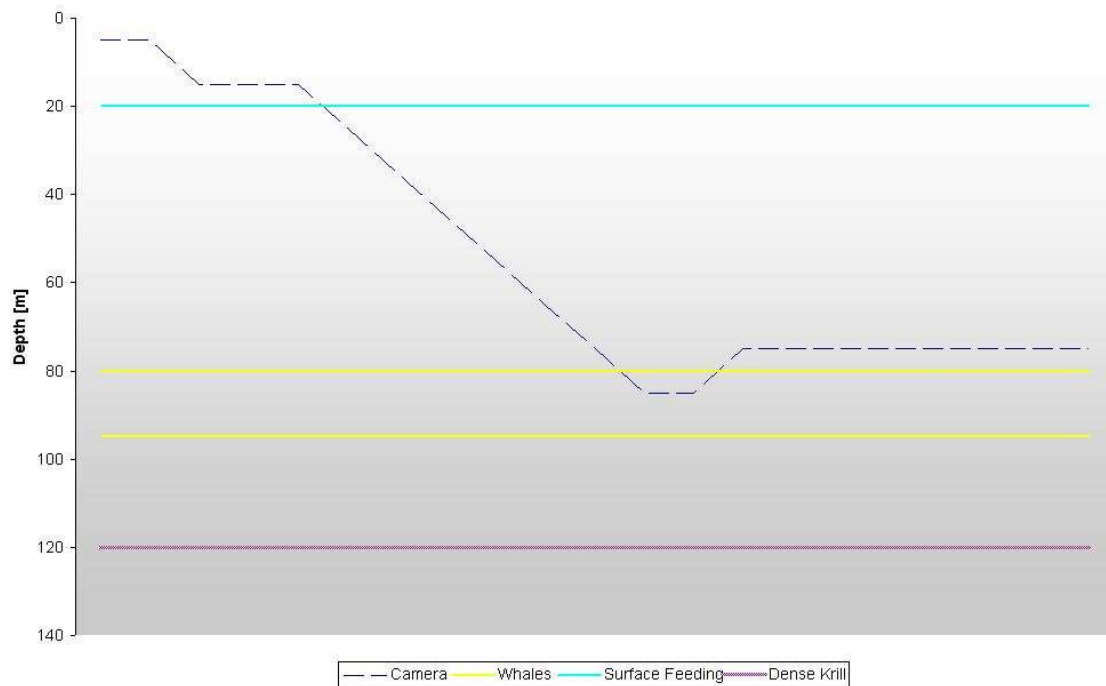


Figure 2-6: Echo Sounder Tracings

However, this graph only represents one single camera dive. It is necessary to have a closer look on diving behavior and the amount of dives in certain depths.

Notice that there are only 662 happenings of bouts recorded, but 4889 dive maneuvers. However, feeding beyond 160 m depth appears not to be very efficient. Nonetheless, with this information in mind, a representative depth must be found to consider boundary conditions for later research on this topic. This depth must also correspond to the deepness where most of the maneuvering is done, as the flipper is naturally adapted best to this depth. This depth is the one where foraging takes place.

Due to its feeding customs, the humpback whale is highly maneuverable, using its flippers to turn and bank at remarkable speed and agility. It speeds up to 2.5 m/s towards their prey while resurfacing at a 30°-90° angle, using their long flippers to uncommonly direct prey into their mouth. Then, the whale swims away quickly with the flippers retracted, suddenly rolling 180° and making a sharp U-turn, again attacking the prey. This maneuver is called “inside loop” behavior and is performed within 1.5 to 2 times the body length of the whale [19].

Another feeding technique is called “bubble net fishing”. Some whales blow bubbles, creating a visual barrier against the prey. Another one or more whales drives the prey against that barrier by vocalizing sounds (chapter 2.2.2). The bubble wall is then closed, encircling the fish. The whales then suddenly swim upwards and through the bubble net, mouths open wide, swallowing thousands of fish in one gulp. This technique can involve a ring of bubbles up to 30 m in diameter [8]. Furrows on the whale’s bottom side might make it easier to soak in a lot of water, while spitting out the water through the baleens and keeping the prey inside.

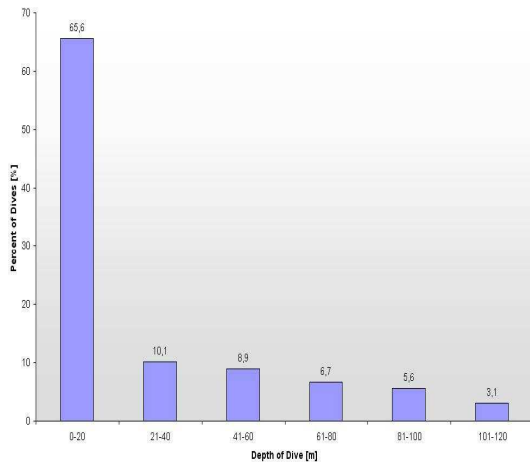


Figure 2-7: Distribution of foraging dives

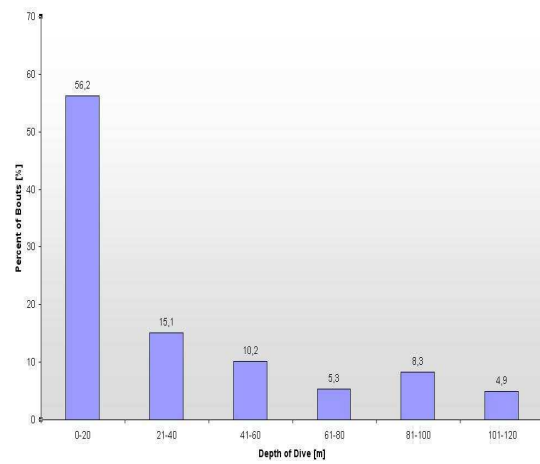


Figure 2-8: Distribution of foraging bouts

Figure 2-7 and figure 2-8 show best on what base a representative depth can be found. Most dives and maneuvers are performed down to 40 m. The exact centre value for all dive and bout maneuvers is 29.5 m. Thus, a medium dive where most likely the flipper is optimized for can be seen at 30 m. This, of course, is only a rough first estimation, as density changes heavily between 30 m and the maximum recorded dive depth of 160 m. However, in some later research the boundary conditions have to change from water to air anyways, so for first considerations a 30 m dive is representative.

2.2.2 Whale Song

Besides this, humpback whales are known for their eager singing underneath the water surface. Scientists assume whale singing is to communicate among one's peers, but also to attract females during mating season. The sounds are not produced congruent to humans, as whales do not have a phonic lip structure. They also do not have to exhale to create sound. The exact mechanism of sound creation is still unclear and a very interesting subject for biologists. [8]

It is assumed that regions involved into sound production are similar to the dolphin (figure 2-9). Frequency varies from 20 Hz to 10 kHz. For comparison, the human hearing range varies from 20 Hz to 20 kHz. There are some patterns noticeable in humpback whale's songs (figure 2-10), for example recurring passages of specific frequencies, but going into detail here would go beyond the scope of this report.

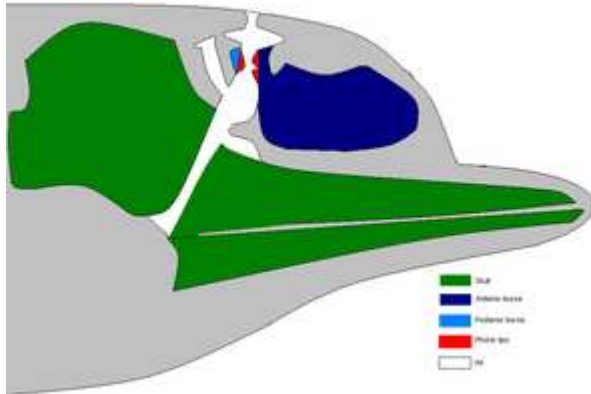


Figure 2-9: Idealized dolphin head showing the regions involved in sound production. [8]

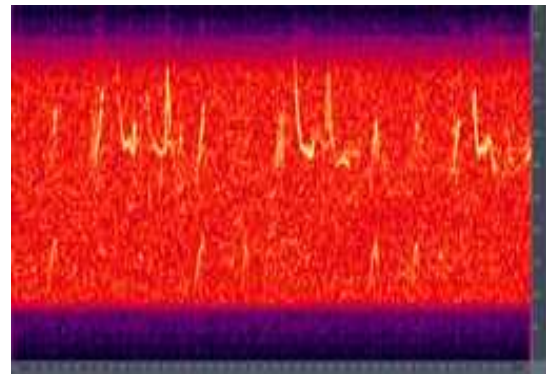


Figure 2-10: Humpback Whale song spectrogram (Listen to Song on CD) [8]

2.2.3 Parasites

It is not assured if jumping out of the water is also due to parasites, as briefly mentioned above. However, the knots on the flipper's leading edge are covered with barnacles and whale lice. These are parasites, living on the whale, whereas the cause for their settlement is still not clear.

Whale lice as shown in figure 2-11 are mostly found close to barnacles. Up to 100,000 whale lice parasites can occur per whale [8]. Sometimes, whale lice settle exactly where barnacles are attached (figure 2-12), scooping out the surrounding area so much that the barnacles fall off.



Figure 2-11: Whale lice, 5-25 mm length [8]



Figure 2-12: Barnacles [8]



2.3 Research Related Details

For this task, some other specific details need to be reviewed before proceeding, to successfully generate a three-dimensional mesh around a humpback whale's pectoral fin and simulate the characteristic flow. In contrast to the chapter above, the details here are described in a more technical manner.

First, the geometry of a flipper has to be stated. Then, in a second step, it needs to become clear how the hydrodynamic flow streams around that flipper in nature. Important key issues are the angle of attack and the fluid's speed for later research on this topic.

2.3.1 The Flipper

As stated above, the flipper has a wing-like, high aspect ratio planform [9]. Its length varies from one fourth to one third of the body length. In cross-sectional view, the leading edge is blunt and rounded, whereas the trailing edge is highly tapered. The maximum thickness can be found from 49 % of chord at the tip to 19 % at mid-span. The thickness ratio averaged 0.23 with a range of 0.20 – 0.28. As already seen, the extraordinary fact concerning these flippers is the leading edge tubercle. These tubercles are supposed to enhance the possible lift, and control the flow over the humpback whale's flipper.

The flipper shown in figure 2-13 shows seven representative cross-sections. The horizontal line represents the chord length, whereas the vertical line represents the maximum thickness. Within this definition, the distance from the leading edge (right side) to maximum thickness is the distance of maximum camber.

The flipper planform is mostly elliptical and a bit tapered. A slight sweep back of around 20 % can be found in some cases, measuring the one-third line relatively to the centerline of the body. There are around ten to twelve tubercles on the leading edge of the flipper, where the largest one can in general be found on one-third of the flipper span. The smallest tubercle is placed close to the flipper tip. The distance between those tubercles decrease from body to tip. Surprisingly, the distance relatively to the span remains almost constant at around 7 % in the middle span of the flipper, displayed in figure 2-15. Barnacles, as shown in figure 2-12, can be found attached to tubercles close to the flipper's tip, but, however, not in the spaces between them.

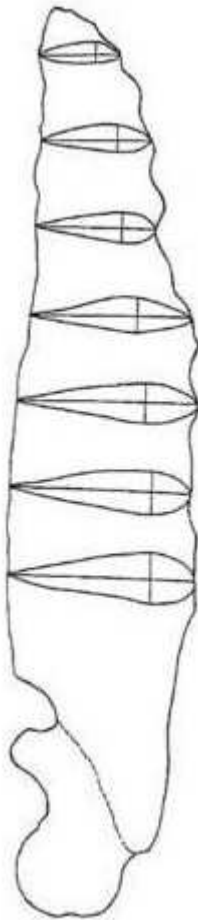


Figure 2-13: Flipper planform with representative cross-sections [9]



Figure 2-14: Humpback whales in Southeast Alaska [1]

Sections within the middle area of the flipper are similar in design to the NACA 63₄-021 airfoil [9]. It is characterized by a streamlined shape, a rounded leading edge and maximum thickness located one-third to one half body length from the trailing edge.

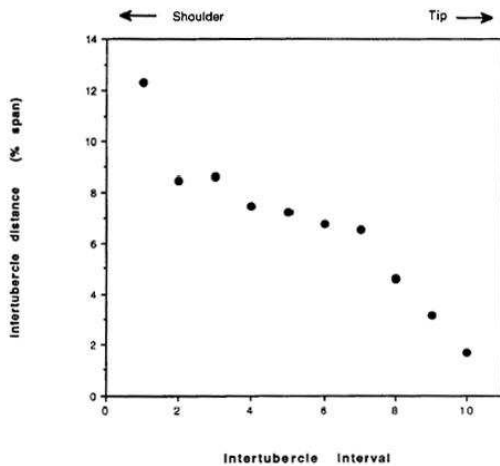


Figure 2-15: Distance between tubercles [9]

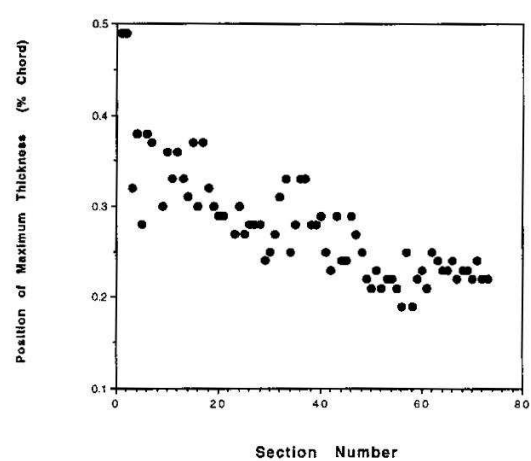


Figure 2-16: Position of max. thickness [9]

However, the position of maximum thickness varies from the flipper's tip towards the whale's shoulder. Figure 2-16 gives an impression on how the position of maximum thickness relatively to the chords changes, while increasing the section number from tip to shoulder.

The tubercles on the flipper seem to exert some sort of boundary layer control on the suction side. They may control hydrodynamic performance on the leading edge, which is the existential justification for this task and further reports following. The humpback tubercles may reduce drag on the flipper, which is stated in later subchapters.

Figure 2-17 shows the skeleton of a humpback whale embedded into its original shape. Hip bones are degenerated, whereas hand bones are completely present. With these bones, it is supposed that the whale can bend the tip up and downwards, stretch the surface and change the angle of the trailing edge through changing the camber.

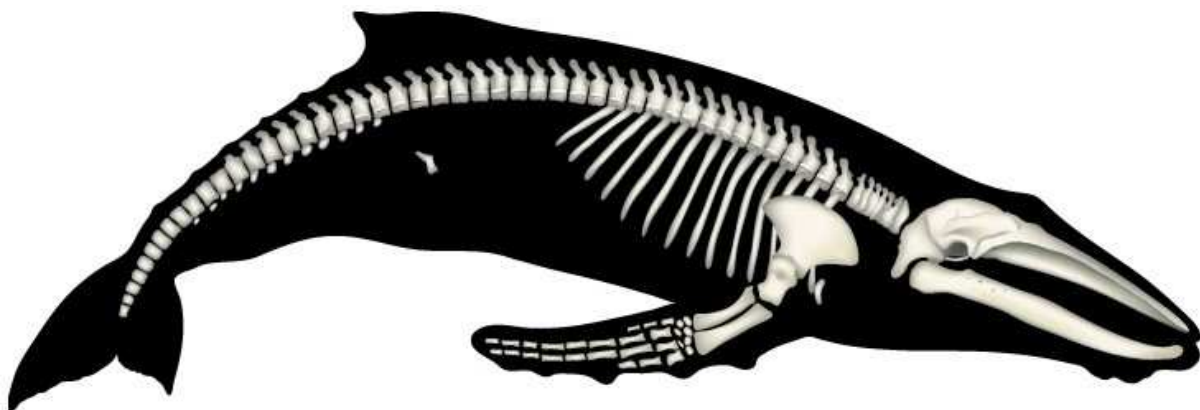


Figure 2-17: Skeleton *Megaptera Novaeangliae* [28]

For now, the flipper is described in detail, but some constraints, for example the oncoming flow, still need to be reviewed.



2.3.2 Hydrodynamic Flow

In general, whales are supposed to be calm and easy going swimmers. Inertia and weight seem to narrow down their possible maneuvering speed, resulting in slow movements and calm positional changes. Surprisingly, their maneuvering speed while feeding (2.5 m/s) and while jumping out of the water (it can be guessed this must be around 10 m/s because of the weight that has to be moved out of the water) is extremely high.

For exact numerical simulation, a typical flow situation must be figured out for calculation. Consequently, the hydrodynamic flow around the pectoral fin is determined in this subchapter.

The flipper's neutral position can be seen in figure 2-18, which shows a humpback whale drawn during straight and level swimming. In several papers [19] it is stated that they are held in a relaxed position forming a 120° - 150° angle to the body's longitudinal axis and a 30° to 40° angle downward to the horizontal line. This is the only way of oncoming flow that is to be considered for later numerical simulations of flow, as of course all the individual movements can not be taken into consideration. It is known that flippers can be moved simultaneously or alternately, symmetrically or independently. Movements rarely occur alone, but in combination with other maneuvers. So, in this case, it is fixed that only the angles of oncoming flow will be considered for later reports.

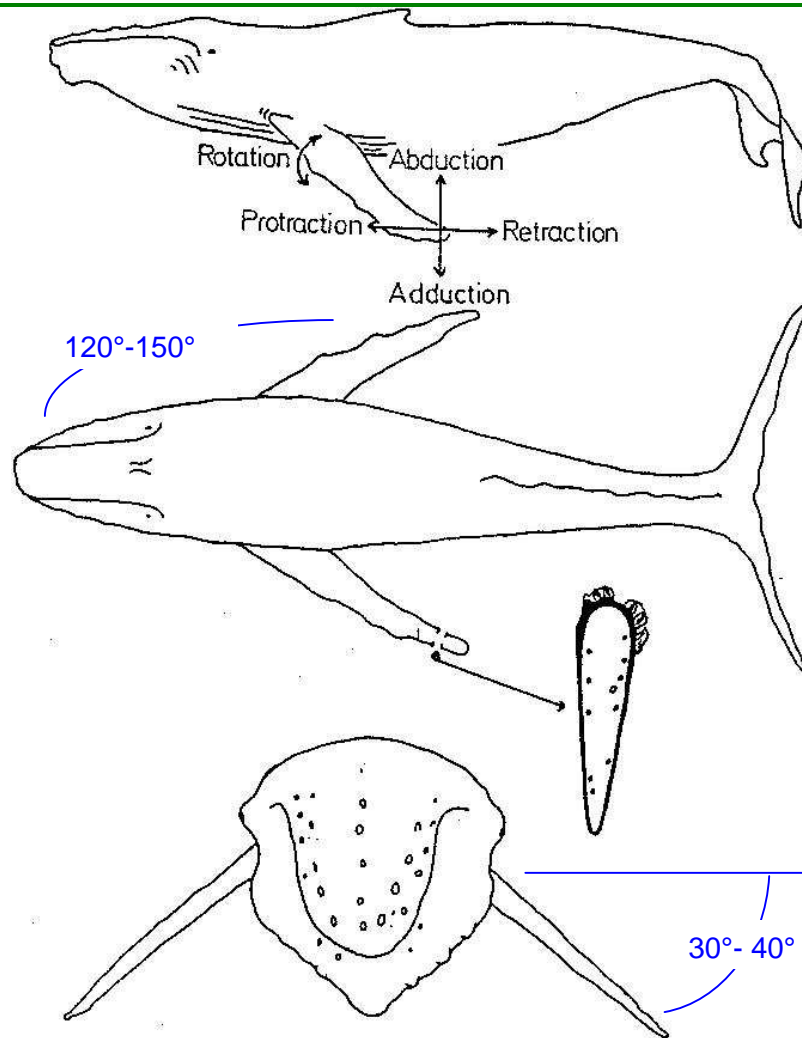


Figure 2-18: Humpback whale from side, top and head-on view [19]

The flipper's skin seems to be very smooth, to support laminar flow. However, under stress it appears to bend, but only to an insignificant degree. This fact is not going to be considered during the numerical simulation, too, as moving or bending objects are hardly executable.

These findings, and the knowledge of maneuvering speed, which can be from 2 to 2.5 m/s, is important for later research on this topic, as it will lead to boundary conditions for the numerical simulation.



$$Re = \frac{\rho v_s L}{\mu} = \frac{v_s L}{\nu} = \frac{\text{Inertial forces}}{\text{Viscous forces}}$$

Figure 2-19: Reynolds Number for Boundary Conditions [8]

However, it is surely necessary to have knowledge about the Reynolds Number (equation shown in figure 2-19) for future purposes. This boundary condition will be well prepared in this report already.

For calculating the Reynolds Number it is:

- v_s Mean fluid velocity,
- L Characteristic length (equal to diameter ($2r$) if a cross-section is circular),
- μ (Absolute) dynamic fluid viscosity,
- ν Cinematic fluid viscosity: $\nu = \mu / \rho$,
- ρ Fluid density.

So, the main thing still missing is the fluid density. The fluid density (around 1 kg/m^3) is almost constant and changes slightly with temperature salt ratio. However, density has to be considered if, in later research, trying to compare these results to numerical simulation within air.

3 State of Affairs

It is assumed that tubercles attached to the leading edge of the pectoral fin have an influence on the boundary layer of the flipper's flow. Thus, for comparison, an overview of similar technologies for controlling the flow around an aerodynamic element has to be given.

3.1 Current Innovations based on Flow Control

As briefly stated in chapter 1.3, some already known innovations that can be adapted to the leading edge are described in this subchapter. There are several leading edge device technologies currently used [2 et al.]. The motivation of this is the economic and environmental pressure of still reaching better aerodynamic values for usual or high lift devices.

As shown in figure 3-1 after some time the optimization progress is decreasing compared to the amount of time spend. Therefore, innovative products are necessary to accelerate the optimization progress.

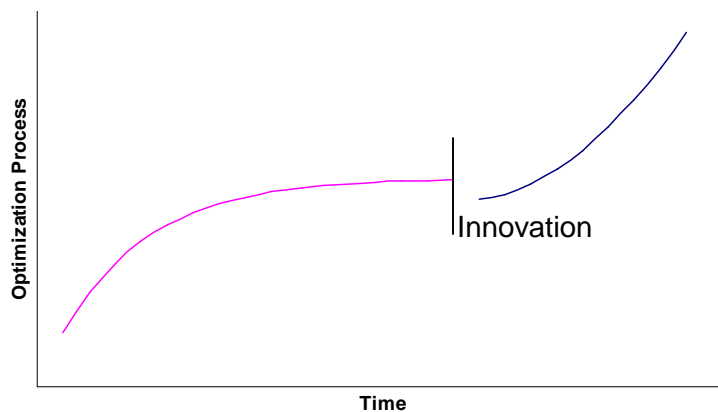


Figure 3-1: Optimization process over time

Due to the large variety of existing flow-control systems, only those relevant for this thesis are named here. In case further investigation would show that tubercles enhance the aerodynamic flow in some flight situations, the efficiency of alternative techniques must be known to evaluate the use of tubercles.

- High Lift Devices
 - i. Variable camber leading edge
 - ii. Fixed slot
 - iii. Simple Krueger flap
 - iv. Folding bull-nose Krueger flap
 - v. Two position slat and three position slat
- Other Multiuse Devices
 - i. Passive vortex generators
 - ii. Air-jet vortex generators



3.1.1 High Lift Devices

The innovations in this sector can again be divided into two major fields of application, namely the leading and the trailing edge. On the wing's leading edge there are known flow-changing devices as slats and Krueger flaps, whereas on the trailing edge many forms and types of flaps are known and briefly described here. Both devices are considered here, as tubercles (leading edge) and bending of the flipper (trailing edge) have the potential to change the flow around the humpback whale's pectoral fin.



Figure 3-2: Commercial airplane taking off using high lift devices [12]

3.1.1.1 Leading edge

Figure 3-3 shows three different leading edge devices, which are described later in the according subchapter.



Figure 3-3: Three different leading edge devices [2]

3.1.1.1.1 Variable camber leading edge

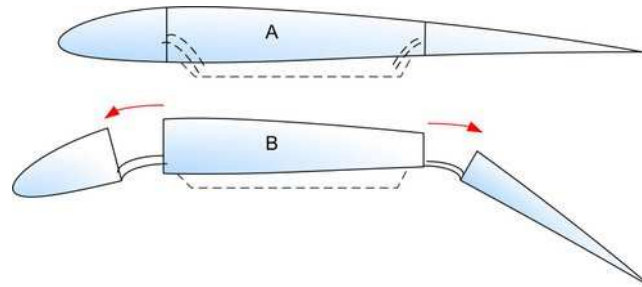


Figure 3-4: Variable camber leading edge [8]

The variable camber leading edge, also known as VC Krueger flaps, bends the main Krueger device and extends the front nose towards the stagnation point. A hydraulic linkage system, with a minimum pressure of four bar, is required to countervail the flow [27].

3.1.1.1.2 Simple and folding bull-nose Krueger flap

Simple Krueger and folding bull-nose Krueger flaps are generally designed with the hinge inside the wing leading edge and connected to the panel with a gooseneck hinge fitting [2]. Additionally, another link must be installed to fold the bull nose into the right position.



Figure 3-5: Krueger flap of a Boeing 737-300 partially extended [7]

The Krueger flap deploys against the forces of the airstream and has a high stowing load at low angles of attack. At high angles of attack, the Krueger flap starts to produce lift. This causes the aerodynamic loads on the airfoil to reverse, which is an unwanted effect in terms of safety. Thus, this device requires high power actuators, which are very heavy, to build up high forces necessary to extract the Krueger flap against the flow.



3.1.1.1.3 Slats

Slats are most commonly used in commercial airplanes to support the other high lift devices on the leading edge. They are mounted on circular arc tracks with two tracks per slat panel. The actual load variation is low as the air loads are normal to the path of deployment.

3.1.1.2 Trailing edge

On the trailing edge, different forms of high lift devices are known. But in this report, only one of them is to be shown here, as it is most commonly used by commercial and military aircrafts.

3.1.1.2.1 Flaps

Flaps lengthen the airfoil in the direction of the trailing edge and therefore broaden the area where lift can develop. However, while flying with extended flaps, flow separation is very likely because of the energy losses in the boundary layer over the long chord length. In this case, slots support the formation of a new boundary layer through transferring flow onto the suction side and thereby eliminating the weakened layer.

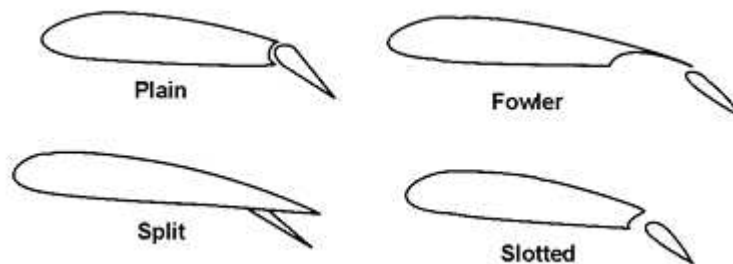


Figure 3-6: Four different types of flaps [8]

3.1.2 Other boundary layer control devices

Vortex generators are a special form of boundary layer control. Besides vortex generators, there are two other forms of boundary layer control mechanisms, to mention them briefly. First, there is blowing, which adds energy to the lower boundary layer by blowing air through slots in the wing surface. This will energize the flow close to the wall and enable it to overcome a larger pressure gradient.

The second form of boundary layer control is suction. This active method of getting rid of the low energy boundary layer is very intensive in cost and power. Very complex systems are needed to prevent the layers above not to mix up with any other layer and ruin the flow. Also, the airworthiness must be secured even in a case of engine failure because a large amount of engine power is used for both, suction and blowing.

3.1.2.1 Passive vortex generators

Passive Vortex generators, as the third method of boundary layer control, are a passive possibility to mix the layer close to the wall with energy loaded air, in contrast to the other active options.

They are essentially small aspect ratio airfoils attached to the wing or other surface, to add vortices into the flow ahead of the separation point, which should therefore of course be after the point where the generators are fixed. These vortices will energize the boundary layer and consequently prevent flow separation. Fluid particles with high momentum in the stream direction are swept along helical paths toward the surface to mix with, and to some extent replace the retarded air at the surface [2] with energized air. While on the one hand the maximum possible angle of attack can be increased, therefore maximum lift can also be increased; drag on the other hand will rise in all angles of flight, too.



Figure 3-7: Vortex generators installed on upper wing surface [Maule Air Inc.]

It has to be critically seen that passive vortex generators cannot be installed elsewhere on the surface. Special considerations have to be made in terms of planform shape, section profile and camber, yaw angle, aspect ratio and height with respect to the boundary layer thickness.

Figure 3-8 shows different vortex generator configurations possible on a NACA RM L52G24 airfoil. These configurations are shown approximately to scale.



3.1.2.2 Air-jet vortex generators

The disadvantage of producing drag in every flight maneuver and every angle of attack can be eliminated by the use of air-jet vortex generators. They can produce strong discrete vortices but have higher momentum cores. Instead of causing additional drag, they can be effective in areas where there is separated flow over the airfoil. As it is an active system, the air-jet vortex generator can be turned off if no use is required or helpful.

Another field of boundary control, namely “acoustic excitation”, is disregarded in this report. Briefly, this is the effect of an imposed sound field on vortex shedding. But, as this is a new field of attention, it has not been examined a lot yet and does not contribute to the main theme of this report, as it is to dimension and estimate possible advantages or disadvantages of tubercle add-ons on airfoils.

Figure 3-9 displays the boundary layer with and without vortex generators. It is easy to see and to understand that at the same angle of attack, the stalling speed can be lower than without vortex generators. However note, that the same airfoil will stall, but at a lower stalling speed than without the generators.

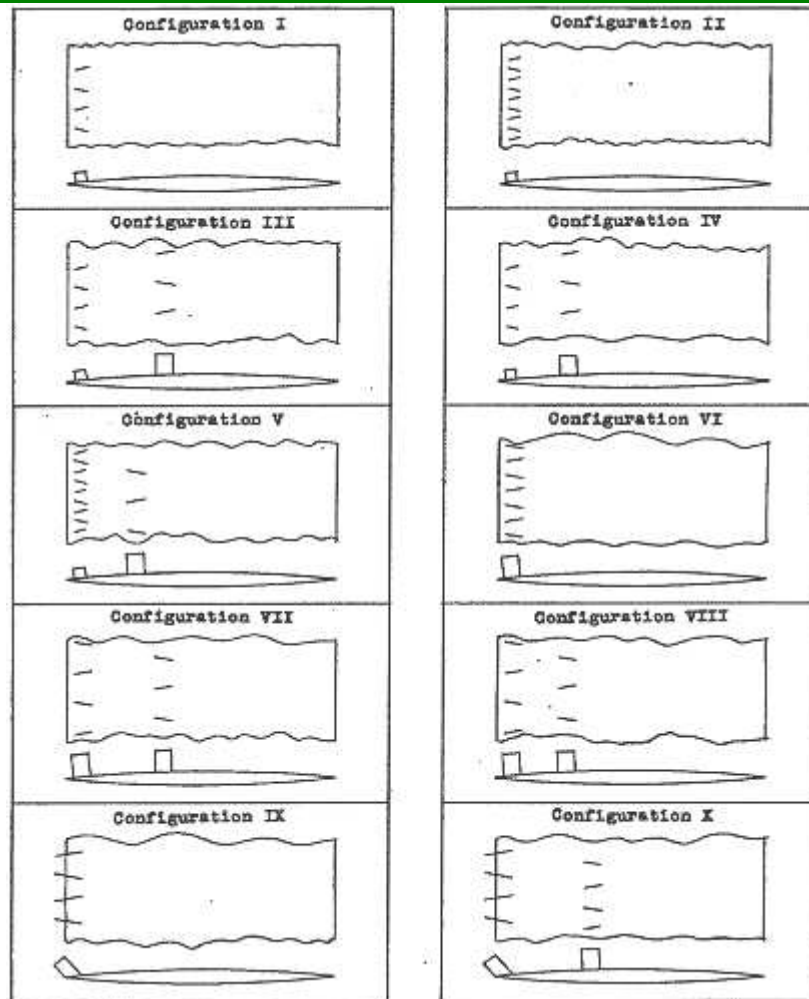


Figure 3-8: Different vortex generator configurations

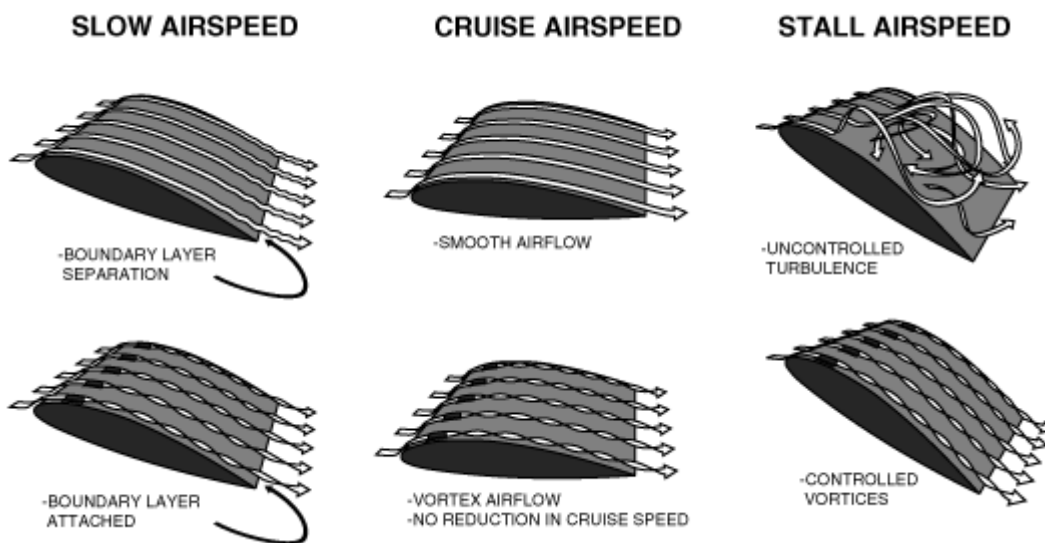


Figure 3-9: Boundary Layer Changes through Vortex Generators [17]



3.2 Previous Research on Pectoral Fins

There has been some investigation on this topic by several other scientists [23], [14].

In detail, it was already considered that tubercles increase maneuverability during prey capture. Thereupon, analysis was done on a finite span wing and on the same wing with tubercles attached.

It was stated that leading edge modifications of streamlined bodies offer cost-effective performance enhancements. A computer supported panel method was developed, to approach the analysis of this statement. A numerical simulation was done on both objects [23].

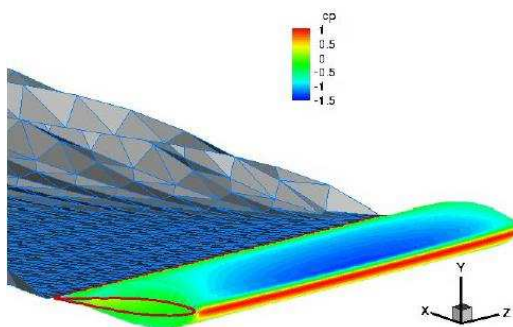


Figure 3-10: Simulation of Flow without Tubercles [23]

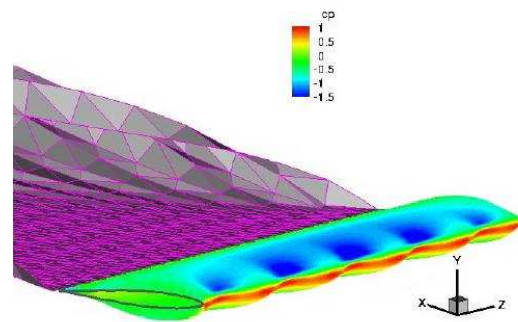


Figure 3-11: Simulation of Flow with Tubercles [23]

The comparison between both simulations showed an increase in lift of 4.8 %, a 10.9 % reduction in induced drag, and a 17.6 % increase in lift to drag ratio (l/d). Tubercles enhanced wing performance at usual to low angles of attack, but did not have a huge effect at zero angle of attack.

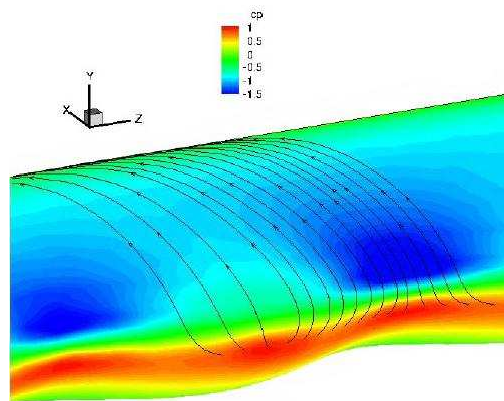


Figure 3-12: Streamlines outside Boundary Layer on Tubercle [23]

Streamlines outside the boundary layer were examined in detail, as the effect on the local pressure was of greater interest for finding aerodynamic loads on the wing. Tubercles may

absorb an 11% increase in drag at a 10° angle of attack. As a result, the flight envelope might be enlarged for better use of the device with tubercles attached.

In addition to this investigation, also real wind tunnel tests were performed within other research [14].

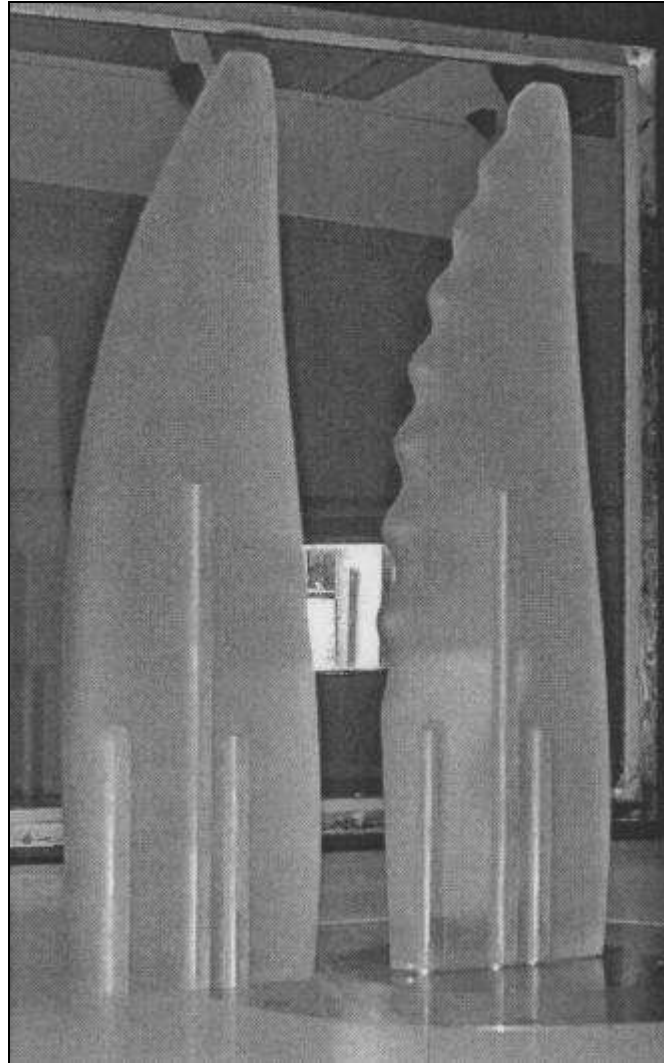


Figure 3-13: Wind Tunnel Models of Pectoral Fins w/ and w/o Tubercles [14]

Two scaled models of a humpback whale's pectoral fin were constructed, one with and one without tubercles attached on the leading edge. The models were based on a NACA 0020 airfoil (20% thickness).

As expected, the flipper with tubercles attached showed a better performance at higher angles. Beyond 11.8° angle of attack, the scalloped flipper produced a 32% lower drag than the smooth model. In a small range of $10.3 < \alpha < 11.8^\circ$ the smooth model showed a lower drag production than the one with tubercles attached. Lift was higher throughout the complete angle of attack range for the scalloped flipper, but still within the range $9.3 < \alpha < 12^\circ$. α_{Stall} increased by 40% to 16.3° angle of attack, while C_{Lmax} increased significantly by 6% to a value of 0.93, so again better values for the scalloped fin. Below $\alpha = 8.5^\circ$, the curve remains almost unchanged.



4 Digitalization of a Humpback Whale's Flipper

As a next step in this report, after identifying and precisely explaining the target of interest, the humpback whale's flipper shall be made available in the ProE CAD Program. This is necessary for further progress in this report, as a numerical net for flow simulations has to be established fitting the surface of a humpback whale's digitalized flipper. To import a surface into numerical simulation tool Ansys ICEM, many data formats can be used. In this report, we agreed on using the IGES format because of good handling qualities. First, the flipper has to be digitalized within ProE, to save and transfer it as an IGES file. This IGES file can later be imported into any CFD or CFX program.

4.1 Preliminary Considerations and Modeling

Every humpback whale is an individual, just like humans. It has its own appearance, own look and behavior. Individuals can only be recognized by detailed observations [20]. The length of flipper and fluke, their color and shape, as well as scars on flipper and fluke are unique for each humpback whale. Generally speaking, this fact makes it harder to digitalize the flipper.

Taking just one picture of a flipper and digitalizing it would therefore be not representative for this project. Thus, it seems to be more reasonable to find a "typical and characteristic" flipper geometry, reflecting the majority of flipper types.

The next task is then to find such a geometry that will fulfill the requirements set up above. This can only be solved by inspection of many photographs, showing humpback whales. Of course, pictures need to be found that will show the flipper in a good angle.

After studying many different pictures, one should have a first overview on repeating details that are equal or similar for several different humpback whale flippers. In chapter 2.3 the skeleton of a humpback whale is described in detail.

The following aspects of real live flipper can not be considered when digitalizing.

- Barnacles attached on the flipper tip
- Flexible stress avoidance movements
- Bending in horizontal and longitudinal direction
- Spreading the bones to enlarge the flipper surface
- Changing the angle of the trailing edge through changing the camber
- Skin state and condition due to stretching and bending and surface impurity

To do a first sketch, of the planform, some proportions have to be copied. Chapter 2.3 can give key references on how to do a first drawing, as it describes structure and appearance of the flipper.

The final step, after observing, identifying and drawing will be to digitalize the created top-view. For this, the coordinates of leading and trailing edge have to be determined and saved in a two-dimensional environment. Finally, this two-dimensional plan needs to be filled in with NACA cross-sections, to upgrade the drawing into a full three-dimensional model. For that purpose, the NACA wing configuration is scaled to fit into the existing flipper top view.

4.2 Drawing the Planform

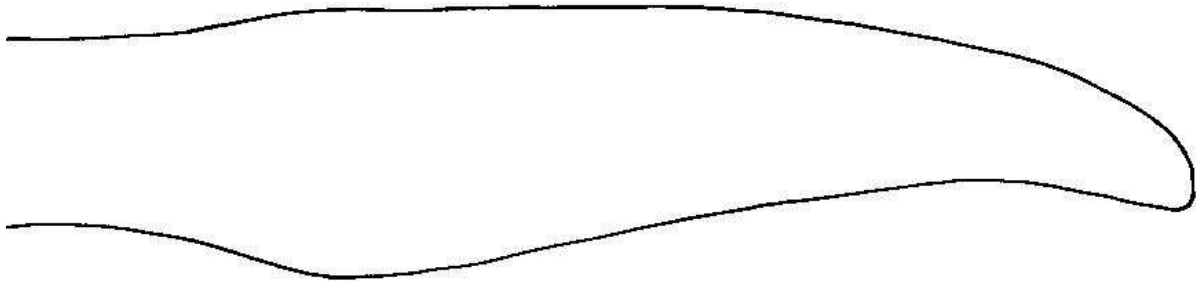


Figure 4-1: Sketch of humpback whale's pectoral fin without tubercles

Looking and comparing with photos, the first drawing is made disregarding the tubercles just to find the typical geometry (figure 4-1).

Then, tubercles were added additionally to the clean sketch of the pectoral fin (figure 4-2). Their position and size was taken from earlier researches on humpback whales and by reviewing photographs.

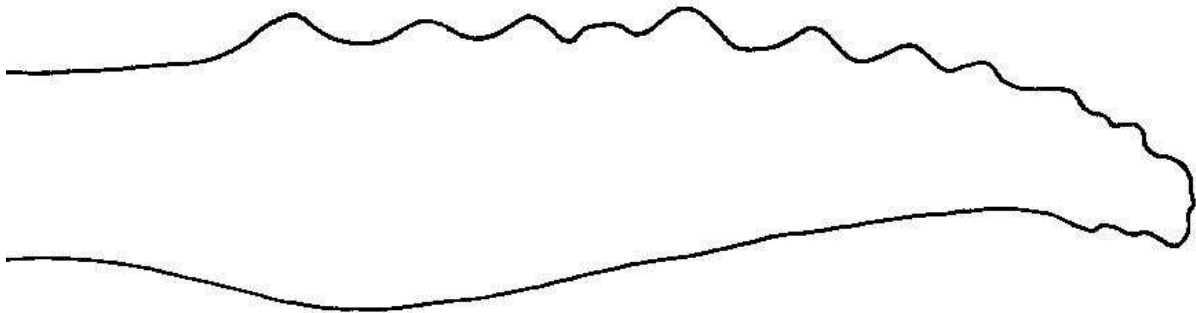


Figure 4-2: Sketch of humpback whale's pectoral fin with tubercles

To complete the drawing exercise, the sketch was colored out in varying grey scales trying to give an impression of three-dimensional depth (figure 4-3).

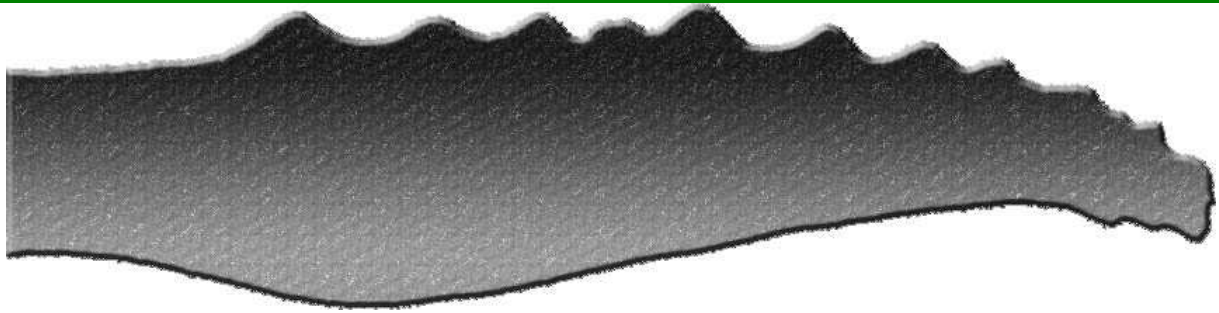


Figure 4-3: Rendered flipper sketch

All drawings were scanned and saved as monochrome bitmaps for further processing.

In general, modern graphic formats compress a file for quicker opening and saving hard disk space. Some formats save changes from one pixel to the other instead of saving each color for every single dot in the picture matrix. For example, if a black picture is saved, the compressed file will use less hard disk space than the bitmap, because there are no changes in color between the dots. On the other hand, quality and resolution might suffer.

However, for this topic saving as bitmap is required, as for retracting coordinates each color for every single dot in the picture matrix is necessary, whereas changes from one dot to the other are irrelevant.

4.3 Reading the Bitmap

At first, the scanned bitmaps needed to be prepared for reading coordinates out of them. Due to scanning imperfections, these bitmaps were inserted into the "hebcad" program to make the drawn lines as thin as possible, and resaved as bitmaps. As coordinates should be read out of the bitmap files, thick lines would cause too many coordinates where there is supposed to be just one line.

As the drawn lines were made as thin as possible, more corrections needed to be made by hand.

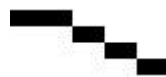


Figure 4-4: Desired pixel course, no doubles, no gaps

Mostly, the lines did not look like the example given above, representing the optimum situation, namely one line, shown by single dots. Unfortunately this is not the case for the whole bitmap. To avoid wrong coordinates, the following rule was agreed upon.

There should be three black pixels at most in a three-times-three pixel square.



Figure 4-5: Pixel course, double pixel



Figure 4-6: Pixel course, gap

Following this rule, the two possible pixel mistakes mentioned in figure 4-5 and figure 4-6 had to be eliminated. This would make a clear and unmistakable finding of geometry coordinates possible. Double pixels had to be deleted, whereas gaps in the course had to be filled.

The program “kkonvert.c” was used [11] to generate a set of coordinates from the bitmap file after these corrections were made.

4.3.1 The “kkonvert.c” BMP-to-Coordinate Converter

The program “kkonvert.c” reads a monochrome bitmap and writes an output file with all coordinates of black pixels within the bitmap. For every black dot the coordinates regarding x and y direction are found and saved. It will sort the database of coordinates in the following way.

There will be two three-times-three pixel squares where there are just two black pixels. These are beginning and end of the drawn line. The list of coordinates is sorted from the beginning of the line, then the following black dots until the end of the line is reached.

The background is just white, whereas the lines drawn should be black. This refers to one and zero bits in a monochrome bitmap.

More information on the converter can be found in the appendix.



Figure 4-7: Coordinates from flipper drawing, without tubercles



4.4 The Flipper's System of Coordinates

To further set a standard on how to describe the fin's coordinates, a system is fixed.

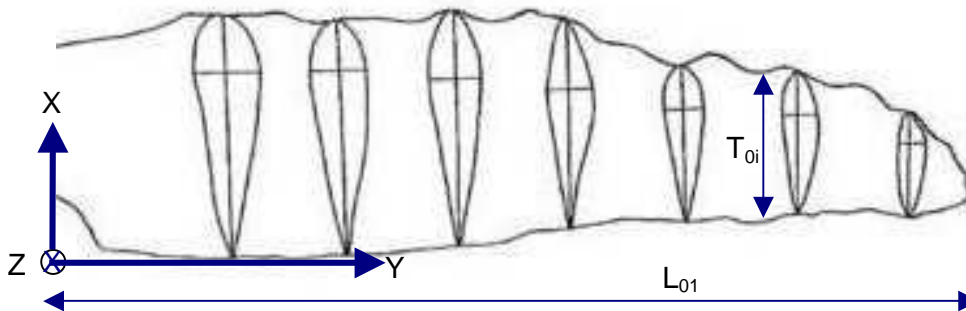


Figure 4-8: Pectoral Fin System of Coordinates, X-Y Layer

Describing the flipper as a whole, figure 4-8 displays the used system of coordinates. The origin is set to the lower left corner of the flipper in a way that no coordinate is negative. The X-axis runs along the flipper's root towards the leading edge, whereas the Y-axis follows the trailing edge. The Z-axis runs downwards. The Flipper length in direction of Y is set to $L_{01}=1$ to scale the results.

T_{0i} represents the chord length of the airfoil profile element within the flipper on position i .

Figure 4-9 shows the system of coordinates regarding each of these airfoils. Within these airfoils, the leading edge is set to $X=0$ and the trailing edge to $X=T_{0i}$. The example shows the first airfoil cut in the flipper.

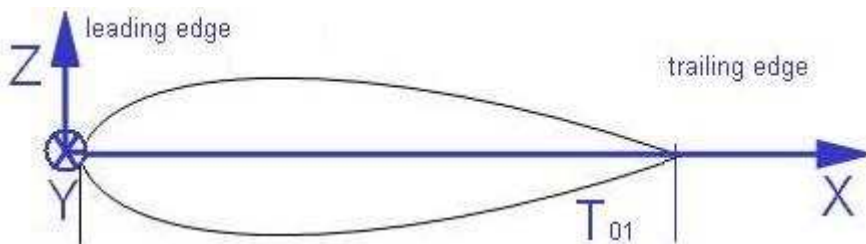


Figure 4-9: Airfoil System of Coordinates

The flipper's volume will be filled similar to a NACA airfoil, which is symmetrical. The line of symmetry is therefore equal to the X-axis running from the leading edge to trailing edge.

4.5 Data Processing in LabView, TecPlot and Excel

The goal of this procedure is to make scalable three-dimensional coordinates readable for TecPlot, ProE or similar. However, there are different problems to solve prior to reaching this step.



First, the length of the flipper, as described by the pixel coordinates, should be scaled to the value of $L=1$, where L is the length of the humpback whale's pectoral fin in the direction of Y .

Then, to fill the two-dimensional planform with a calculated volume, as briefly described in the subchapter above, for every Y the chord in the direction of X must be known. To find this chord length, the distance of two points having the same ordinate has to be calculated from the table of pixel coordinates generated by the kkonvert-software.

The coordinate system has to be defined as described in the subchapter above. With all the topics stated above cleared, the three-dimensional flipper can be formed out of the two-dimensional flipper draft and the NACA airfoil.

There are two procedures in LabView which will help finding those chords lengths.

- Finding coordinates:
This procedure reads coordinates out of a text file, in this case "Profil ohne Tuberkel-Koordinaten.txt", and writes the chord with every (x, y) coordinate into a specific output file.
- Deleting data:
This procedure will then reduce the amount of (x, y) coordinates to a reasonable number (e.g. 40). This will be the data for the cuts and sections mentioned in figure 4-12.

However, there is a specialty to realize in TecPlot. Within this program, the decimal point must be a point as such, whereas the versions of Excel and LabView used within this report need a comma as decimal point. A program for changing the format of these values to fit as an input file for the specified programs is Ultra Edit, which can change points to commas automatically.

Now, the coordinates arranged in LabView need to be reviewed in Excel, to make sure that the geometry is at least like a pectoral fin.

Table 8-1 shows a list of coordinates to describe the humpback whale's pectoral fin, without considering tubercles. The Y coordinate can be found in the Y column. The $X1$ column comprises the leading edge, whereas $X2$ is the trailing edge. The chord can be found as the difference in length between $X1$ and $X2$ in the direction of X .

Figure 4-10 and figure 4-11 give a graphical output of the table described above. For the Fin without tubercles, only 20 cross-sections are necessary. They are marked by small dots. These dots can also be found in the picture underneath. In figure 4-11 more dots are required to give an appropriate image of tubercles on the leading edge. When using not enough dots, the shape of the pectoral fin changes significantly.

However, the digitalization of a fin without tubercles is the main concern in this matter, as only this type of fin will be covered with a mesh in the first place.

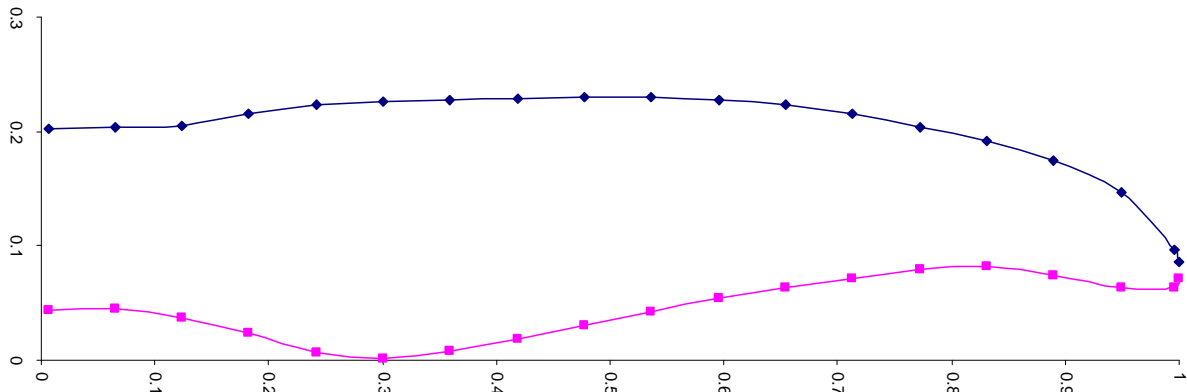


Figure 4-10: Excel Output for Pectoral Fin without Tubercles

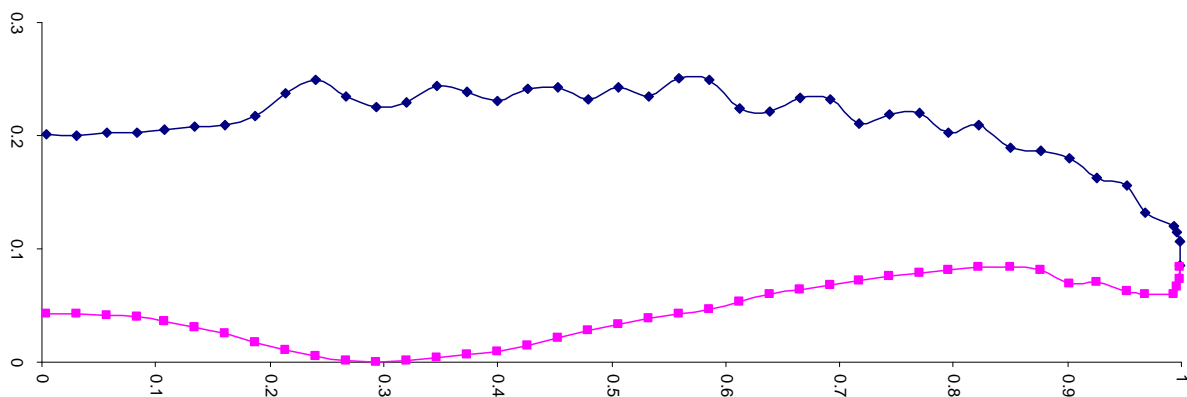


Figure 4-11: Excel Output for Pectoral Fin with Tubercles

4.6 Generation of a Third Dimension

The main idea of generating the Z-values to fill the two-dimensional drawing is to use a thickness-function corresponding to a NACA airfoil and extract a Z-value for every X-value of the chord. This has to be done in three steps. First, a matching NACA airfoil has to be found and values describing this airfoil have to be identified. Second, these NACA coordinates have to be scaled to fit every position within the flipper data. Finally, the Z-Values can be calculated from the chord length.

4.6.1 Finding the NACA airfoil

Biologists found that the thickness of a pectoral fin averages from 0.20 to 0.23 percent of chord length [9]. These examinations were done on stranded whales measuring the flipper. Obviously, this would lead to a minimum NACA 0020 airfoil. However, during own reviewing of photographs of living humpback whales, this airfoil was found too thick. A NACA 0012 airfoil suits better in terms of thickness, corresponding to these photographs. Thus, the NACA 0012 airfoil is taken for generating the third dimension.

Exact data describing an NACA 0012 airfoil can be found from reference [29].

As the thickness is going to be generated regarding chord length and regarding the NACA 0012 airfoil, the characteristics of this airfoil need to be clear. The encryption for NACA 4 digits series is quite easy. The first digit stands for maximum camber in percentage of chord. The next displays the position of maximum camber in $1/10^{\text{th}}$ of chord length. Finally, the last two digits represent the maximum thickness in percentage of chord.

With this knowledge exact airfoil data for a NACA 0012 airfoil is available. In addition to that, the needed chord lengths are also known, as they can be calculated from the coordinates stored in table 8-2.

4.6.2 Scaling the NACA Wing Design

Scaling the NACA 0012 airfoil is simple if as in this case values for the flipper chord length (x) are known for each part of the fin (y). So, it is $x=f(y)$. The following set of equations will solve the problem.

$$X = s \cdot x_{NACA} = x_{Fin}$$

$$Y = y_{Fin}$$

Table 4-1: Set of Equations for NACA scaling

For easier scaling, the pectoral fin is cut into several sections. For each one of them, the thickness of the volume can be calculated with table 4-1.

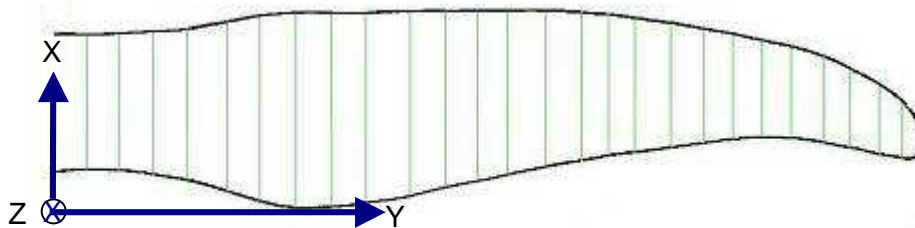


Figure 4-12: Cuts and Sections within Pectoral Fin

This information of two- and three-dimensional data can now be used for further procedure.

4.6.3 Calculation of Z-Values

At this point of study, a two-dimensional flipper is generated and all coordinates for the trailing and leading edge are known. However, the information of thickness is still missing. The third dimension, meaning thickness in correspondence to the chord length, needs to be determined.



As in another way stated above, the transformation can be described easily by the following set of equations.

$$x_{3D} = s \cdot x_{NACA} + x_{Fin}$$

$$z_{3D} = s \cdot z_{NACA}$$

$$y_{3D} = y_{Fin}$$

Table 4-2: Set of Equations for chord scaling

The difference to table 4-1 is that here, s is the length of the chord dependent on Y.

TecPlot will now calculate with 19 cuts in the direction of X (J), will fill in 141 NACA airfoil points (I) and will scale the fin to a length of L=1.

As figure 4-13 and table 4-3 may provide, the 19 cuts are now filled with points to display the volume in the direction of Z.

TITLE="Pectoral Fin without Tubercles"		
VARIABLES="x", "y", "z"		
ZONE I=141	J=19	F=POINT
0,187175	0,006066	0,000201
0,18516	0,006066	0,000481
0,182016	0,006066	0,000911
0,178754	0,006066	0,001345
0,175405	0,006066	0,001781
0,171992	0,006066	0,002213
0,168535	0,006066	0,002641
0,165048	0,006066	0,003061
0,16154	0,006066	0,003473
0,158018	0,006066	0,003877
0,154487	0,006066	0,004271
0,150949	0,006066	0,004655
0,147407	0,006066	0,005029
0,143863	0,006066	0,005393
0,140318	0,006066	0,005747
0,136773	0,006066	0,006089
0,133228	0,006066	0,00642
...

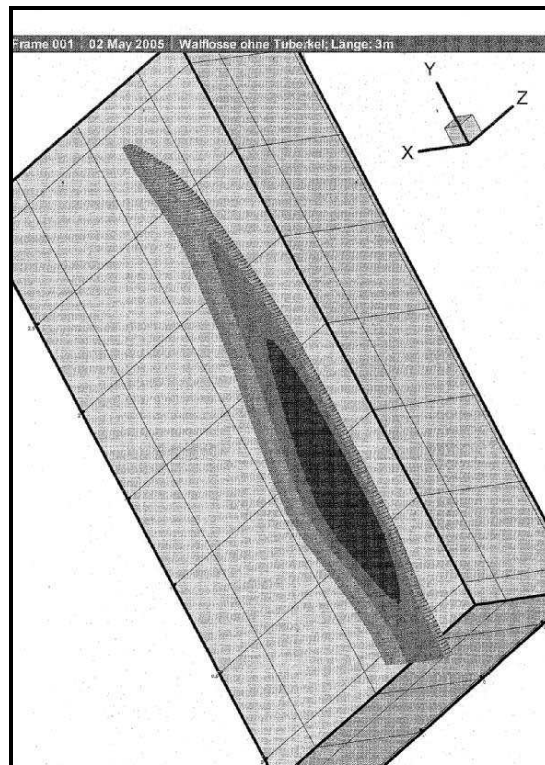


Table 4-3: TecPlot Database Abstract

Figure 4-13: TecPlot Fin Printout

State of knowledge is now that data is available for points describing a pectoral fin in three dimensions without tubercles.

To better reproduce these methods of digitalization, some errors and mistakes found are written down hereafter. Their solution might be a hint for similar problems in other fields.

4.7 Troubleshooting ProE

To solve problems importing data into ProE, LabView output files were inserted into an Excel spreadsheet. There, the amount of decimal places were reduced, followed by saving this file not as Excel integrated format (XLS), but as a commonly used ASCII text file (TXT). To keep the information of rows and columns, used in Excel to separate the data within the sheet, tab stops should be used.

Using the Program UltraEdit, both files, the LabView output and the file changed through Excel, seem to be the very same. But the problem importing this file to ProE is now gone. However, there is another problem that came up during the digitalization process.

In some of the graphical outputs within ProE some errors could be seen.

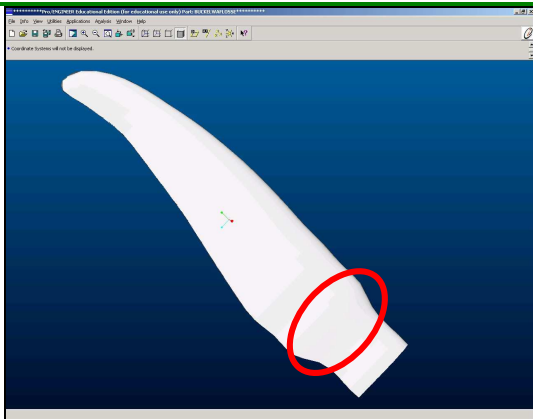


Figure 4-14: Error in Pectoral Fin Surface, ISO View

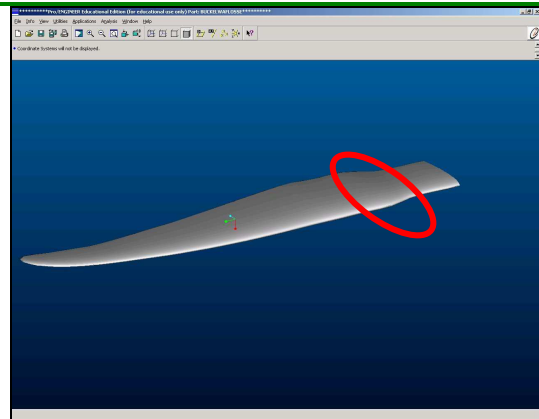


Figure 4-15: Error in Pectoral Fin, Head-On View

To get rid of this error in surface creation, the points close to this error had to be corrected by hand. The reason for this error is simply a line change in importing the coordinates.

However, after eliminating the errors, buckling and angles in the marked section, screenshots of the digitalized flipper without tubercles is displayed underneath.

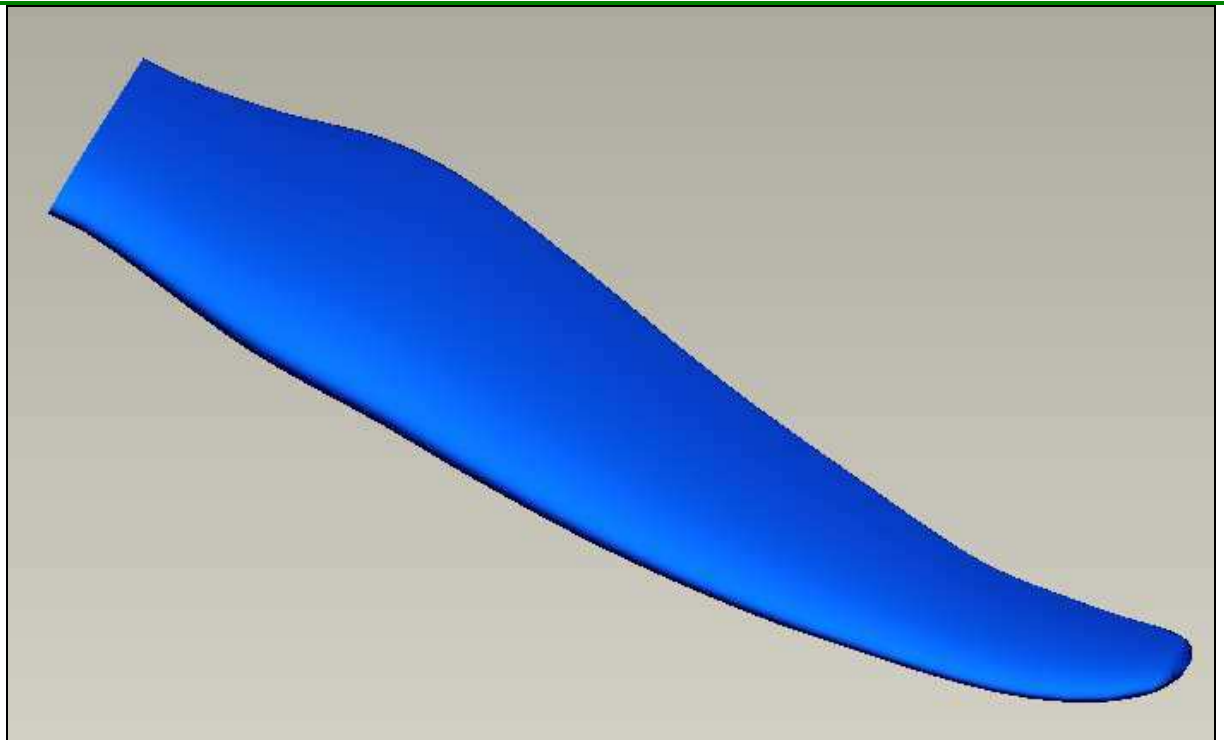


Figure 4-16: Screenshot of Pectoral Fin without Tubercles



4.8 Generation of Digitalized Pectoral Flipper with Tubercles

In this subchapter, the specialties of generating a digitalized pectoral fin with tubercles are addressed. Briefly those matters are described which are different to generating a pectoral fin without tubercles.

An approach had to be found to model the tubercles onto the leading edge. Three options were taken into account. First, the bitmap with tubercles could be scanned and the Z-values could be calculated as above. The problem was seen that with this method, the volume would be thicker than the original pectoral fin in those areas where tubercles are attached, as tubercles lengthen the chord. This would result in a wavy surface, not at all representing the original flipper. Second, a clean flipper could be taken and tubercles could be simulated with attached paraboloids of revolution (circular paraboloids). This looked very artificial and not congruent to the original flipper, too. Third, it was considered to take the clean flipper and calculate the thickness from its chord length, and form the tubercles by hand fitting them best to the scanned image. This method yielded the best results and will be detailed in the following paragraphs.

At first, the LabView programs will extract the coordinates of the flipper chords to a TXT file. But here, in this case, 19 sets of coordinates are not sufficient. Instead, much more layers in the closer area to tubercles are mandatory for an exact display of the pectoral fin.

The primary question is therefore to find out how many cuts are necessary to represent a most conform pectoral fin according to the original image, without having to deal with too many coordinates.

This is a typical trial and error problem. The iteration was started with around 50 sets of points, but at the end it turned out that 42 sets are sufficient for a successful description.

The following approach on how to find coordinates for a pectoral fin with tubercles is made.

At first, the LabView program for creating coordinates has to run on the bitmap without tubercles again, considering the minimum distance of one cut to the other to properly display the tubercles. The output of this has to be shortened so that only coordinates of the leading edge and chord length are left.

Now, the X-coordinates of the file containing the flipper with tubercles have to match those within the file not containing tubercles. If these X-coordinates match, the according chord length from the data file containing the non-tubercle version can be noted.

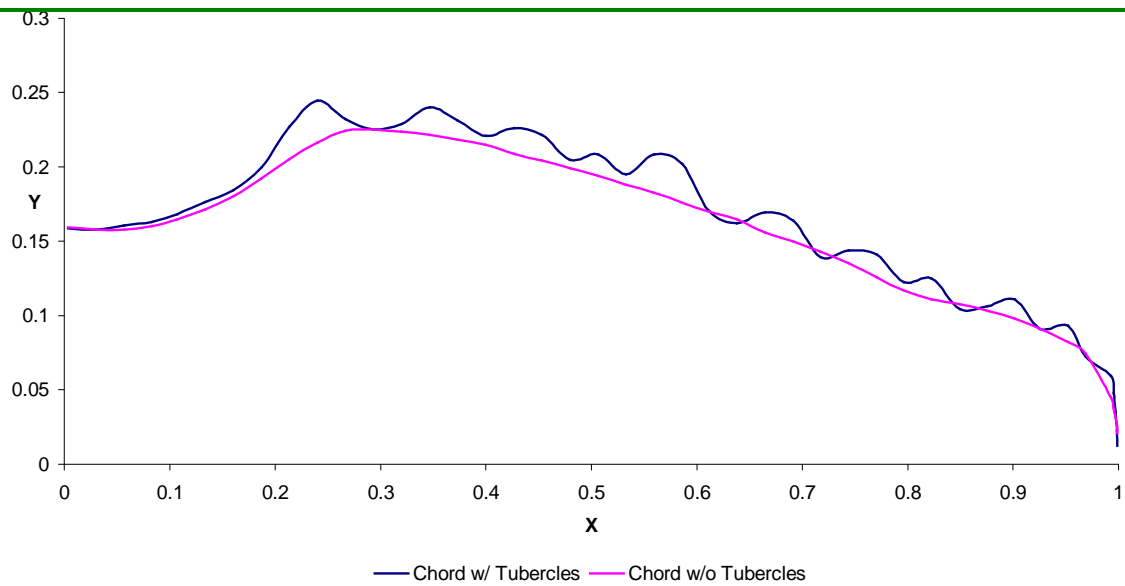


Figure 4-17: Confrontation Chord Length w/ and w/o Tubercles

From this data, the according NACA 0012 airfoil thickness can be determined, and scaled regarding the chord length of the corresponding X-position of the digitalized pectoral fin without tubercles. This thickness is therefore the same for the version without as for the version with tubercles.

During performing this procedure one of the following problems can occur. Either, the according X-coordinate can not be found, or the according X-coordinate is not exactly equal to the X-coordinate in the other file. The troubleshooting on this is first to cut the last decimal numbers but 4 and to scale the pixel interval to $1 = 8.65E-4$.

Also, the maximum distance between two X-coordinates was set to 0.000550. This value is sufficient to find a corresponding value for all 42 sets of coordinates needed for the digitalization of the pectoral fin with tubercles.

Still, these value need to be checked by hand, as some failures can still occur.

Again, this file has to be imported into Excel, to check geometry and steadiness of the surface. This check can be performed in two sheets.

Within the first sheet, all coordinates are copied into three columns. These coordinates are the X and Y coordinate, and the length of the chord. The first check therefore is whether all rows are filled out so that no coordinate is missing. A chart was set up to ensure that the geometry is correct.

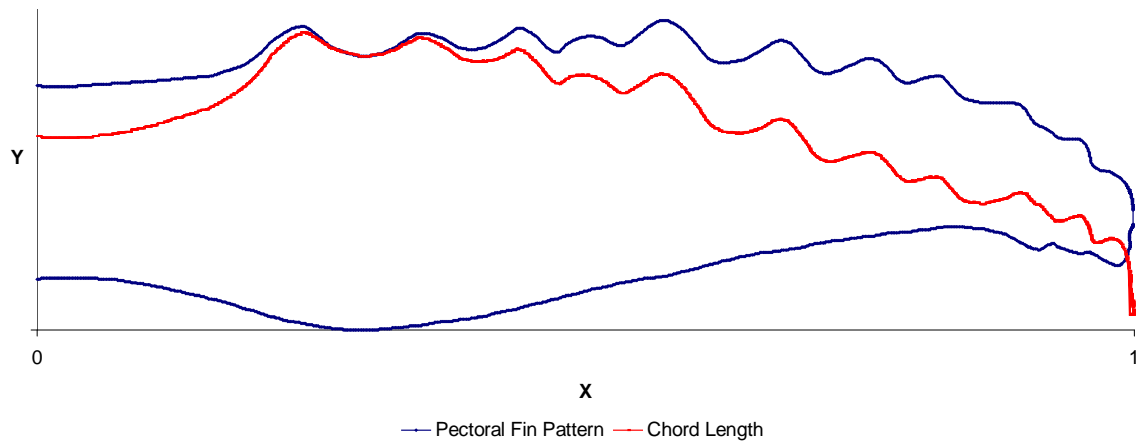


Figure 4-18: Pectoral Fin Pattern and Chord Length including Tubercles

Figure 4-18 displays the pectoral fin pattern constructed out of those coordinates. It also displays the chord length drawn over the flipper width.

This is now necessary to follow the check up to sheet two. The Problem is that the pattern in figure 4-18 can not be described as a function, as on X-value can be assigned to two Y-values. Thus, another way of describing the pattern has to be found.

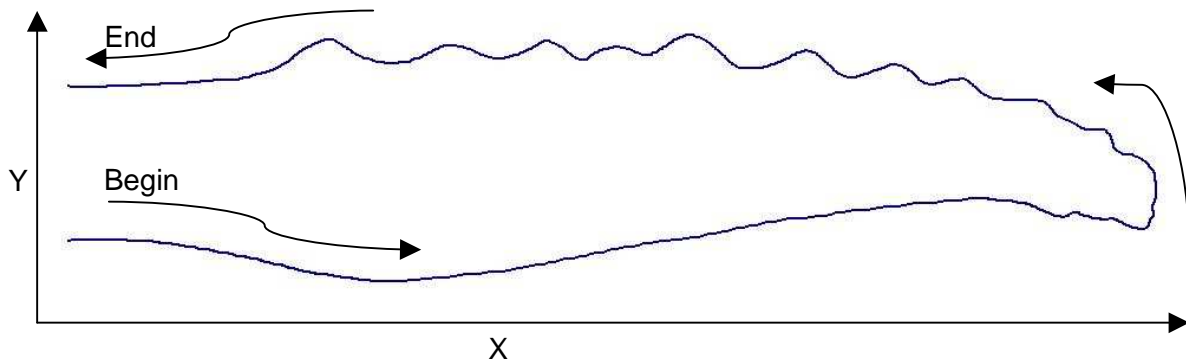


Figure 4-19: Sequence of Coordinate Data around Fin Pattern

The direction and sequence of the set of points from the top of the list to the bottom is shown above. But now, to describe the flipper's pattern with a function, it is constituted that only the flippers leading edge is described as a function for $X=0..1$, and the trailing edge is then concluded out of subtraction of the chord length. For this, the chord length is being subtracted from the Y-Values, where the X-Value is being retained.

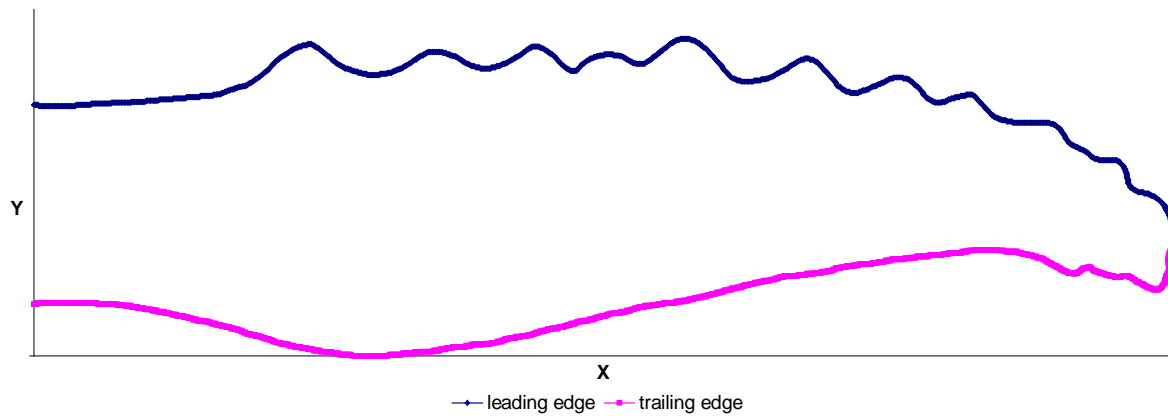


Figure 4-20: Leading and Trailing Edge of Pectoral Fin with Tubercles

Everything signed in blue is directly plotted through the coordinates given, whereas the other half is calculated through the subtraction mentioned above.

4.9 Import into ProE Wildfire 2.0

Preliminary actions to this import are as described above and summarized hereafter.

Files containing the flipper's coordinates must be present in a *.pts format. This file can be obtained by the LabView procedure explained in the precede subchapter. Through this file, the X and Y origin of coordinates and X and Y distances can be measured. A cautious look has to be given to the decimal separator, which needs to be a point instead of a comma. This is due to the fact that ProE was developed in the US and therefore needs some correction on mathematic spelling within our metric system.

The remaining procedure of succeeding in finding correct input data is analogue to the instruction above. However, further attention still needs to be given to length, width and scale. Also, the correct correspondence to the abscissa, ordinate and z-axis needs to be carefully watched.

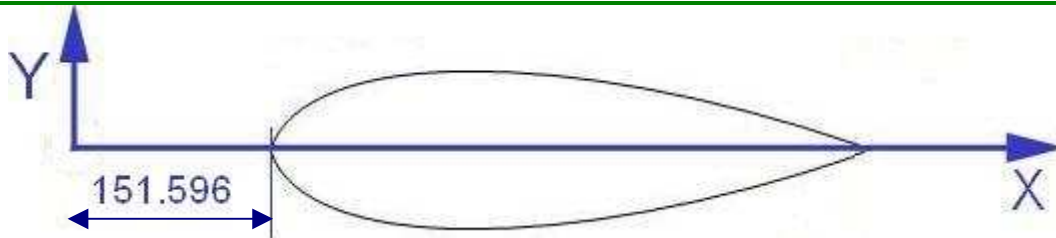


Figure 4-21: Example for axis situation and coordinate value.

Table 8-3 is giving an example of ProE input data, marking a pectoral fin with tubercles. Note that section thirty-two and thirty-three have the same X-position, however, this seems to be reasonable and alright with regard to a steady surface.

Nevertheless, it seems to be a greater effort to import so many sections, as ProE was making trouble importing every spline at once. Besides programming errors, this may most likely happen because of capacity problems on the used hardware. So, the fin was cut into two parts and added into ProE separately. The first run was made to be section one to seventeen, then eighteen to thirty-one, followed by the remaining sections.

Section forty-two is the corresponding value for the flipper's tip. It may be left out for a better graphical solution.

4.10 Export as IGES File

The export from ProE into an IGES file was done setting the following options.

The attributes were set to "smooth", the front plane direction was set to "Z-Axis" while the sketch plane was left on default.

While reading the sectional data file, the scale ratio was left to "1" and no rotation was set.



While using the tool "Toggle Section", the last section was not toggled to not use it. The system of coordinates was fixed for measuring purposes. Distances between the individual points were inserted.

Finally, the output file was set to be an IGES file and saved as such.

Finalizing the digitalization, the flipper with tubercles will show like the screenshot in Figure 4-18.



Figure 4-22: Screenshot Pectoral Fin with Tubercles



4.11 Simplifications and Troubleshooting

Before creating a mesh around the pectoral fin, the simplifications partially stated within the text above are summarized so that reproducing the findings of this work is made easier.

- **Individuality**

As all humpback whales are individuals, an appropriate method of mapping a universal flipper needs to be discovered. Many pictures and images of flippers in different angles were sorted, to get an idea of shapes, measures and ratios. However, this indicates that the later digitalized flipper can not be an exact copy of the original fin and its flexibility, but an idealized and partially simplified version.
- **Pixel Course**

Drawings can be read in easily, but naturally different line weights are used while drawing by hand. So, the pixel course read in by programs used for this step has to be adjusted. This procedure is well described in the according subchapter above.
- **Number of sets of coordinates**

While reading the bitmap, a lot of coordinates for points within that bitmap are extracted. Reducing the points will result in better efficiency and quicker establishment of the digitalized fin. However, having not enough points will lead to a bad resolution and possibly to unsteadiness and errors in the later model.
- **Decimal Marker**

During importing and exporting data files, some file formats had to be carefully observed. This is among others the cell spacing, the separation of columns (e.g. with tabs or blanks) and the decimal marker. However, some programs require the metric system, some the US system. The user should be well aware of the required data format, as many following errors can be avoided.
- **Mapping Tubercles**

Considerations in mapping tubercles were not only done in the direction described above. It was also taken into account to emulate tubercles by attaching a paraboloid of revolution (circular paraboloid) to the fin. However, the used method seemed to be most efficient.
- **Limitations by Computer Resources**

Importing the data file into ProE, certain limitations due to insufficient computer resources have to be considered. In this case, not all the points could be imported at once. Thus, the amount of points inserted into ProE was split into two parts. The reunion of both parts had to be done very carefully as a proper surface is mandatory for further development.
- **Limitations by Computer Software**

Decent movements, bending, tightening the skin or the adjustment of the flipper to irregular flow can not be regarded in this subject, as ICEM CFD can only cope with static, non moving and non morphing model data. These calculations would go beyond the scope of this report.



5 The Mesh

A grid around the humpback whale's flipper is established with the use of the software "ICEM CFD" by Ansys.

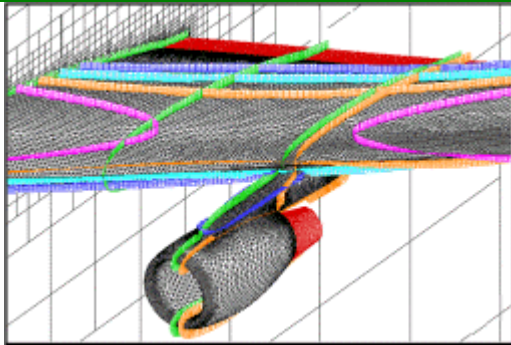


Figure 5-1: Hybrid Grid [4]

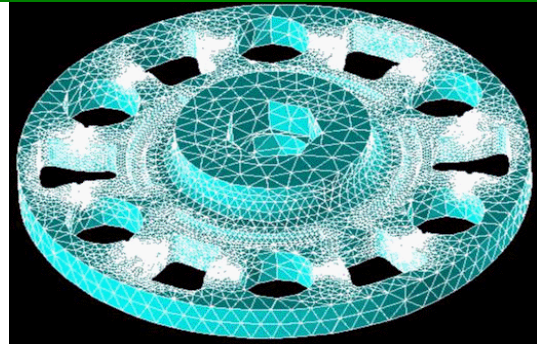


Figure 5-2: Tetrahedron Grid [4]

There are three types of grids available in ICEM. Hexahedron Grids (figure 5-4) are used for three-dimensional simple surfaces. Grid edges are aligned to the coordinate plane. The second type is the tetrahedron grid, an unstructured type of mesh, shown in figure 5-2. This grid is best for complex surfaces with better resolution in the boundary layer including the option to calculate heat transfer. The last, as a mixture of both, is the hybrid grid as in figure 5-1. This grid needs professional skills to be created, the grid itself is very complex. Consequently, the hexahedron grid is chosen for meshing, as this grid is the best for numerical analyses.

First, it needs to be explained out how a hexa grid works and what key issues need to be considered. The theory of generating a hexa mesh is a further topic within this research.

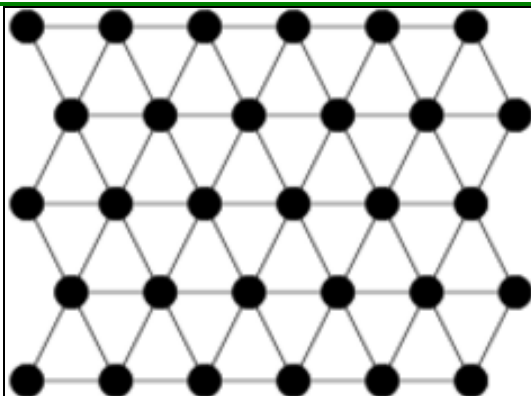


Figure 5-3: 2D Hexa Grid [24]

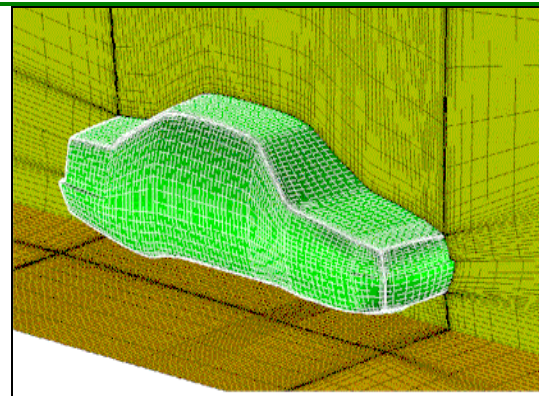


Figure 5-4: 3D Auto Hexa Grid around Car [4]

Figure 5-3 shows a 2 dimensional hexa grid. Every node is connected to six strings. In three dimensions, as shown in figure 5-4, every cell consists of six nodes, as hexa is Greek for "six". However, the car shown is processed with Autohexa, a utility made by Ansys to generate hexa meshes quickly and automatically. This utility is unfortunately not usable for this report.



Therefore, a hexa mesh needs to be generated around that digitalized fin by hand. In addition to that, for better results in further computing, a much finer grid should be established in the proximity of the fin. This results in more computing complexity, but will deliver much better results than just the ordinary hexa mesh.

Later in this report, some sentences will be presented on exporting this mesh into the CFX solver, and what problems arise during mesh generation.

5.1 The Hexa Mesh in Theory

Hexa is a 3-D object-based, semi-automatic, multi-block structured and unstructured surface and volume mesher [3].

To generate a hexahedral mesh, a block topology model can be generated to fit directly on the underlying CAD geometry.

However, there are two ways to generate a mesh within the program. On the one hand, block topology can be used. A three-dimensional block model can be created, similar to the original topology. Edges, curves and faces of that block can be adjusted to fit geometry and surfaces. On the other hand, the geometry can be used directly. Advantages out of symmetry and transformations can be taken.

5.1.1 O-Grid

Creating an O-grid is an option to improve quality of meshes. For very complex geometries, the mesh around the geometry surface can be condensed to better fit the block topology to the surface. O-grids can be internal and external. An O-grid can be established in several ways, using an automated procedure, which is unfortunately very inaccurate, inside and outside O-grids, as said, and O-grids with a face to let the O-grid pass through the desired block face. O-grids can be re-scaled to fit other geometries even after generation, if they are built up automatically. In fact this only works for very easy surfaces and surface changes, but for complex surfaces this is not possible after all.

As a side effect, O-grids can generate orthogonal mesh lines at an object boundary. The use of this is not considered further in this report. In general, creating an O-grid is setting constraints in the proximity of geometry and is independent from the mesh type.

The procedure of creating an O-grid is schematically described in the following figures. Figure 5-5 illustrates the initial block. In figure 5-6, an O-grid is inserted into the initial block. Figure 5-7 shows the same block with an O-grid, with the O-grid and the initial block sharing a face.

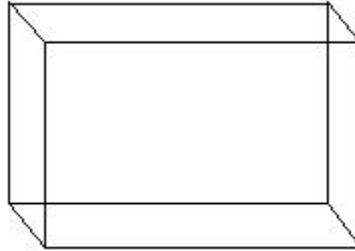


Figure 5-5: Initial block

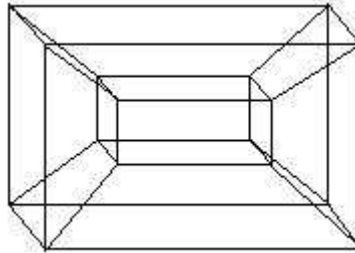


Figure 5-6: Block with O-Grid

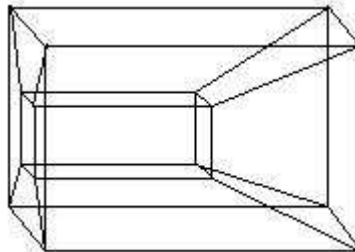


Figure 5-7: Block with O-Grid and including a face

5.1.2 Edge-Meshing Parameters

Edge-meshing parameters within CFD offer “unlimited” flexibility in applying user specified requirements, bunching the net at the desired spot. However, this option is very limited in terms of export and readability by following CFX programs. Edge meshing parameters have to be carefully chosen not to receive various failures in CFX.

5.1.3 Time Saving Methods

There are several methods which are designed to save time while generating a hexa mesh, like surface smoothing and volume relaxation methods.

Any block can be refined or coarsened during the mesh building process. Especially in areas of extremely high or low angles, these refinements can lead to better meshes. The replay option can be used to repeatedly perform similar actions. This replay option was often used in this report to cut blocks and reconfigure them, as many blocks had to be taken to fit the surface.



There are many other time-saving options available in CFD, but only those are listed here, which are used in this meshing process. For example, there are symmetry based algorithms, link shapes and adjustability. It is referred to the according user manual for more information.

5.1.4 Hexa Database

The hexa database contains the grid elements. It consists of the following entities, making it easier to select or deselect wanted items for later treatment.

- Points: x, y, z coordinates
- Curves: trimmed or untrimmed NURBS curves
- Surfaces: trimmed or untrimmed NURBS surfaces
- Vertices: corner points of blocks, at least eight that define a block
- Edges: a face has four edges, whereas a block has twelve edges
- Faces: six faces make up a block
- Blocks: volume made up of vertices, edges and faces.

This shows that geometry is very parametric listed within CFD, so that hexahedral grids can be easily remeshed on the modified geometry or parameters on the selected entities can be changed easily.

5.1.5 Unstructured and Structured Mesh Output

The unstructured mesh will give an output where all common nodes on the block interfaces are merged.

For solvers like CFX that accept multi-block structured meshes, the structured mesh output option can produce a mesh output file for every block in the model.

However, this number of output files can still be controlled by setting a fixed number of output files and merging any of the other nodes at the block interface.



5.2 Meshing the Pectoral Fin

The process of meshing a humpback whale's flipper includes creating blocks around the geometry, assigning solid and fluid material, creating an O-grid for better resolution of the boundary layer, setting up mesh parameters and exporting to a solver.

5.2.1 Blocking

One of the main steps prior to building a hexa mesh is setting up the blocking. The blocking strategy is commonly used to create a hexa mesh.

The main features of blocking are:

- O-Grids
- Edge Meshing Parameters
- Time Saving Methods
- Mesh Quality Checking
- Mesh Refinement/Coarsening
- Replay Option
- Symmetry
- Link Shape
- Adjustability

Although not all of these features are used during this topic, they are named here for reference. Those used for this topic are explained hereafter.

The generation of the blocking starts with importing the geometry file. Figure 4-16 shows this geometry. The blocking is generated through split, merge, O-Grid definition, edge/face modifications and vertex movements. Because of the complexity of the used methods, standard preferences shown in tutorials are used in the beginning, gradually adjusting them to the actual task.

For this meshing, the tutorial "meshing a wing" is used. Figure 5-8 shows the geometry delivered in this tutorial, and the blocking created around this geometry. Blocking is associated to the geometry surface already.

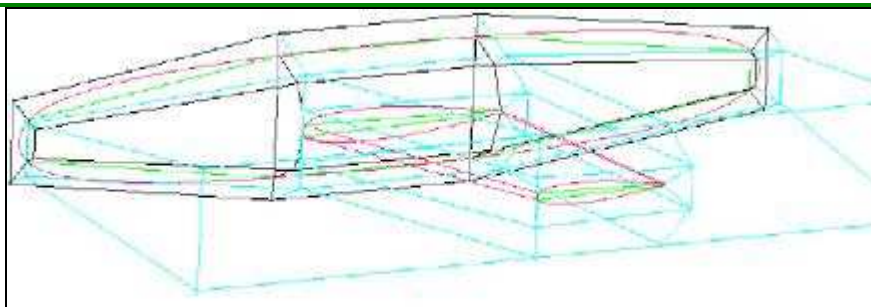


Figure 5-8: Blocking Strategy around wing



The blocking for the pectoral fin is created in a similar way, around the edges and corresponding to the surface.

Starting the blocking, a huge block is set up around all entities. This is supposed to be the volume, in which the fluid will be simulated. The block is named “Live” and it is proceeded to the next step.

Within ICEM, all points, curves and surfaces are made visible. As blocks are symmetrical to the coordinate system, it is now obvious that the initial block has to be split into smaller blocks to better cover the geometry. Splitting the blocks can be done by using prescribed points to exactly mark the cut. Unfortunately, the IGES geometry consists of curves and surfaces, so that points have to be attached accordantly.

This major block is now split after all points are set at those corresponding places expecting a change in fluid dynamics. These places are supposed to be around tubercles, at the flipper’s tip and shoulder. The splitting of the block is done by the “split block” feature using the method “prescribed points”.

Further splitting is done by using the “index control”. This is a powerful tool to cut block edges in a way that one block can be divided easily into two parts, keeping two opposing edges of the original block as reference edges and cutting the other two edges into halves, into a ratio determined by calculation or dividing the edges at a position simply determined by mouse click.

All blockings have to be associated to those surfaces which have to be meshed, to set the meshing parameters. In this case, problems occur as associating to surfaces is not possible due to irregularities found in the geometry (possibly wholes on the flipper’s tip or shoulder, or due to the division while importing the data in ProE). As the specific reason can not be found, a manual procedure of associating the blocks to points and curves is performed. For this procedure, additional points have to be attached onto the surface again.

The “Associate Vertex” button is used for this step, but as mentioned, not all vertices can be moved by automatism. As seen above, automatism is not helpful for this task in general. As a consequence, many vertices have to be moved by hand with the corresponding dialogue.

5.2.2 Assigning Material

For solving this mesh with a CFX, material and fluid must be defined. This is done through creating parts, as shown in figure 5-9.

The option “create parts with block” is used to assign the material to those blocks inside the pectoral fin. These blocks are marked and named “SOLID” in the corresponding dialogue.

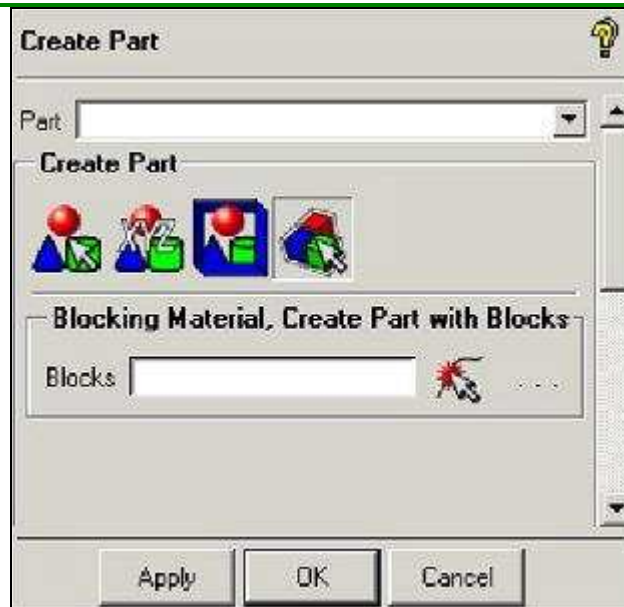


Figure 5-9: Creating Parts Interface for defining Material

5.2.3 Creating the O-Grid

In this step the O-grid is constructed around the whale's flipper, i.e. around the volume named SOLID during the assigning material procedure.

As described already, the O-grid captures the boundary layer around the geometry.

Now, all blocks not being within the LIVE layer are switched off, so that the SOLID blocks can be selected more easily. All visible faces have to be surfaces of those blocks. The O-grid is then created using the split block interface, while choosing the option "select face".

5.2.4 Mesh Parameters

Some mesh parameters have to be set before generating the mesh. For this, the “surface mesh size” window is run in the mesh interface. Values are changed according to figure 5-10. All surfaces available are selected.

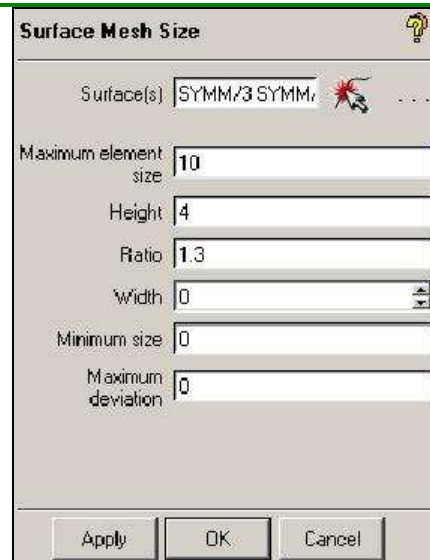


Figure 5-10: Surface Mesh Size Dialogue Screen

As a last step, within the pre-mesh parameters, all mesh sizes are updated.

Through pre-meshing, the outcome can be seen prior to meshing the whole pectoral fin. Some extra options are toggled, in order to change the mesh slightly to find better outcomes.

5.2.5 Mesh around Pectoral Fin without Tubercles

Building up the mesh around the pectoral fin without tubercles is not a trivial task. As described in chapter 5.2.1, the geometry file itself cannot be used offhand, as additional points, curves and surfaces have to be added and adapted often prior to meshing. Points and curves have to be added for cutting and associating blocks and faces, therefore to create a pre-mesh onto the geometry. After these increased efforts, generating a mesh fitting most of the requirements is possible.

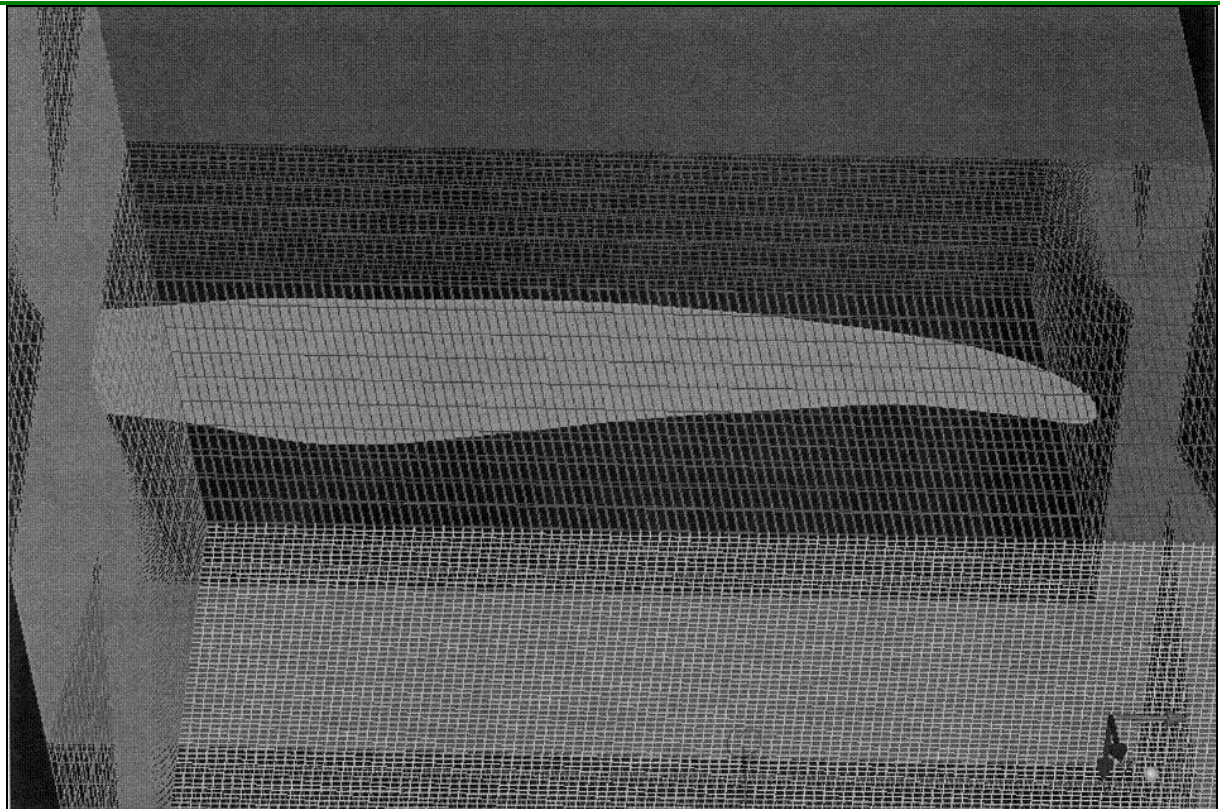


Figure 5-11: Mesh around Pectoral Fin

The O-grid around the pectoral fin is pictured in a light grey. This O-grid will help solving reactions in the boundary layer around and close to the fin.

Irregularities seen expeditiously in the mesh in figure 5-11 are as follows.

- Constrictions at the flipper's tip and root
 - These constrictions narrow the mesh at the areas of tip and root. This is wanted as a tighter mesh is more accurate and increases quality of the numerical simulation.
- Narrowing of the mesh above and underneath the flipper
 - This narrow mesh results from the tight mesh on the flipper's top and bottom surface. Due to symmetry, the small hexa vertices convey to the outer limit of the mesh. A narrow mesh at these areas does not affect the results of the numerical simulation in a negative way.
- Constrictions of the mesh at the wake of the flipper
 - Narrowing the mesh on the flipper's level improves simulation results of the flow behind the pectoral fin's trailing edge.

Saving this as a structured mesh, it can be exported into the numeric flow solver CFX, which is delivered within the Ansys ICEM package.

5.2.6 Export to CFX

Once the mesh is generated in ICEM, it can be exported into a solver. CFD can be performed on two types of meshes, which are both supported by ICEM. The first type is an unstructured mesh, like solved by STAR or CD; the second is a structured mesh, solvable by CFX or TASKFLOW.

In this case, CFX is used, thus the mesh is transferred to be a multi-block structured mesh. After the appropriate solver is chosen, boundary conditions are added with “Boundary Conds”.

First, a region within the family boundary conditions has to be created. The region is named “OUTLET”, to define an outlet for flow calculations later on. Other regions can be defined as desired.

Finally, the file is exported to CFX. Unfortunately, many errors occur in the file created. These errors are not visible in the mesh created with ICEM, and arise only in the mesh after importing into CFX. The actual cause of these errors is not known. It is assumed that earlier errors while associating blocking or establishing the pre-mesh have an influence on these failures in the mesh. It remains unclear, why these errors are not visible in ICEM CFD. Another cause might be the export interface or the protocol version while exporting to CFX.

Figure 5-12 shows the imported mesh in CFX. The weaknesses can be spotted in the zoom (figure 5-13). Heavy irregularities in the mesh covering the flipper’s trailing edge and inconsistencies on the flipper’s tip make it impossible to perform a flow simulation.

As said above, the exact cause for this problem is not known. To avoid the problem could thus be easier than to solve it. Consequently, a new approach to generating the mesh has to be done from scratch. This includes the digitalization of the flipper and saving the geometry in a file format making it possible to use points on the surface with ICEM CFD. Blockings can then be cut and associated for a hexa grid more efficiently.

Another approach is to use an alternative mesh type. After extensive thoughts the tetrahedron grid seems to be suitable. This is therefore recommended in chapter 6 and can not be done in this thesis due to the limited time frame.

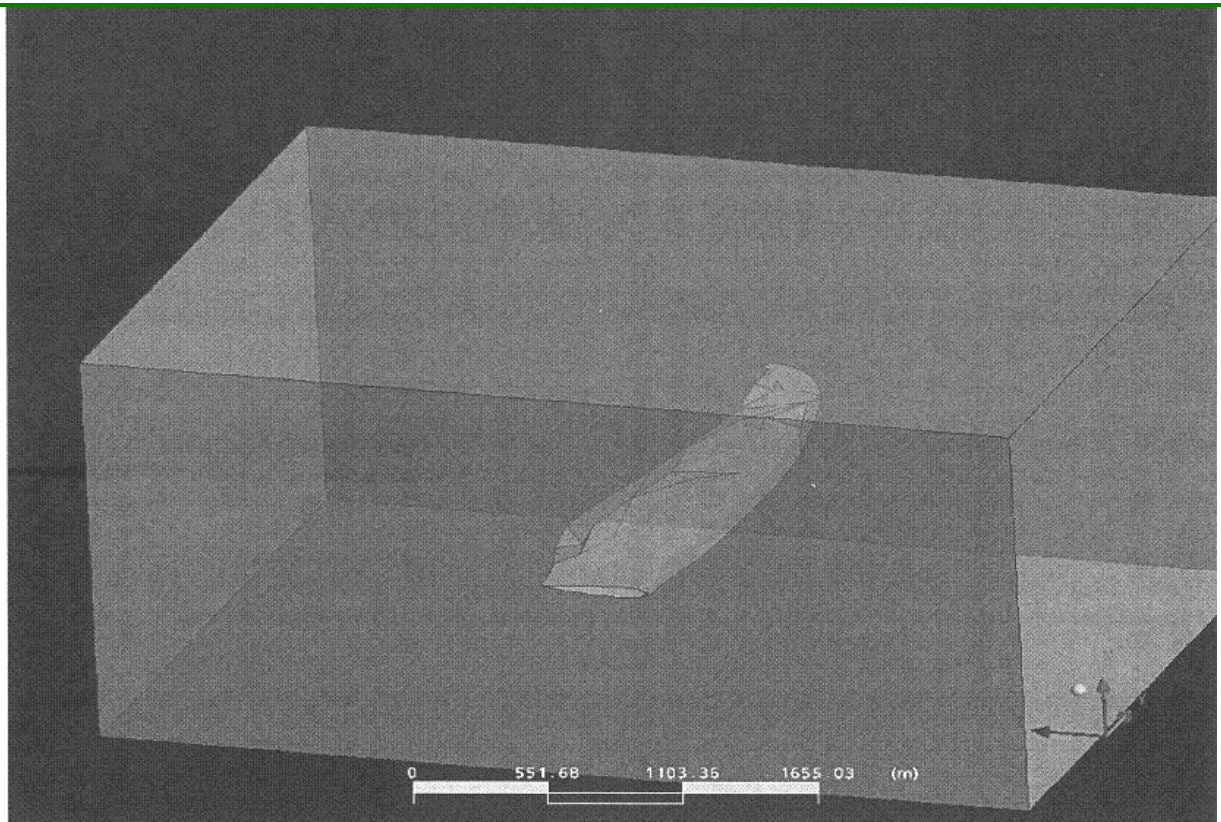


Figure 5-12: CFX Imported Mesh

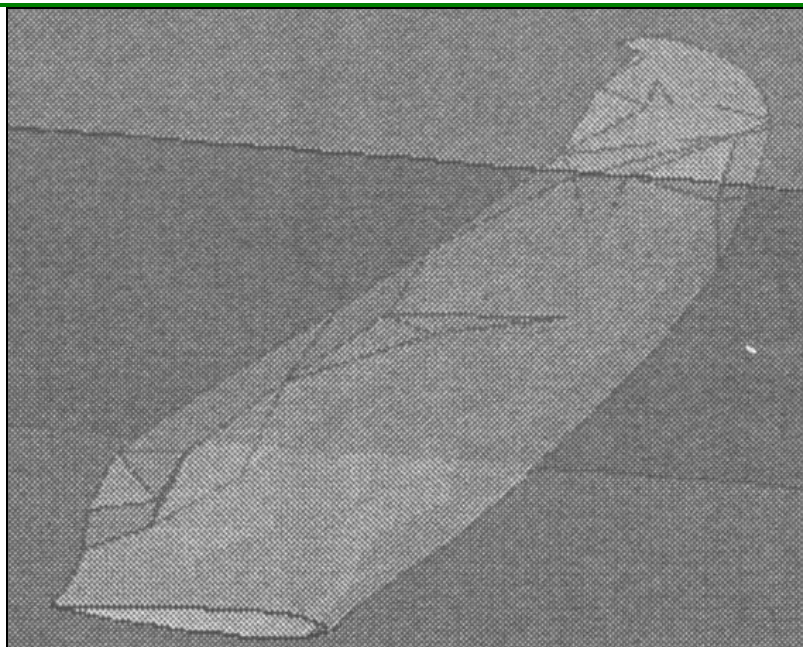


Figure 5-13: Zoom on meshed Flipper in CFX



5.3 Troubleshootings and Problems

Some troubles experienced in this subchapter are stated here for convenience.

- **Missing License of Autohexa**

The Autohexa feature helps meshing an existing geometry automatically. However, it can not be said if this feature would have worked correctly in this case, even with the experience gained through the tutorials setting up a hexa mesh is still complicated. Nevertheless, an automated meshing tool for tetrahedron grids is available, which is the reason for recommending this type of grid in chapter 6.
- **The Blocking Strategy**

In order to set up a hexa mesh, blockings have to be installed around the flipper. Several complex problems are experienced within this procedure. Blocking edges are automatically aligned to the coordinate plane. The flipper's curves are obviously not aligned in a straight and 90 degrees order. This results in many small blocks to map the surface of a pectoral fin. Using the version with tubercles, every tubercle has to be set up with its own block making this version impossible to mesh. In the end, a lot of blockings are created, which is good for mesh quality, but bad for overview and efficiency.
- **Associating Block Faces**

All blocks have to be associated to the surface. However, the fin's surface can not be identified as such by ICEM. Thus, blocking faces can not be linked properly with those surfaces. Therefore, a lot of additional points have to be added to the surface by hand. This is a very inefficient method of solving this problem, but turned out to be the only successful one. All other methods, e.g. finding holes or trying to find the surface automatically, proved effectless. After creating many points on the surface, the blocking edges and faces can be associated with these points.
- **Mesh Quality**

Installing a regular hexa mesh does definitely not result in good mesh quality. An O-grid has to be created as well. This created grid is compressed at the tip of the fin a lot, thus, all the grid lines at that point are moved and compressed as well. This results in better mesh quality around the fin, which is wanted because of boundary layer effects, but affects the resolution close to the outer edges of the mesh, which is regarded as minor in this matter.
- **Node Connection**

The error message "no node in grid file" is finally eliminated through setting up the material properly and not only pre-meshing, but meshing the whole system at once. It is a result of no volume, but only surface meshing.
- **Export to CFX**

Exporting the mesh depends on the used solver, chosen in the according dropdown menu. Still, some mesh errors occur in CFX, which are not accounted anymore as the mesh type changes in further research.



6 Conclusion and Recommendation

Analysis of humpback whale’s flippers in wind tunnel tests show improvements in maximum lift and reduction of drag compared to a clean flipper, and suggest that further investigation in flow simulation is lucrative to understand the concrete physical mechanisms of flow control through tubercles attached to the flipper. These mechanisms could not be determined within this thesis. Instead, a typical pectoral fin is successfully identified and through complex methods digitalized. This part and the evaluation of errors in ICEM took up most of the time.

The mesh in chapter 5 is found not sufficient for numerical simulations to be solved by CFX, as it has flaccidities in steadiness and consistency. Re-meshing would go beyond the time frame of this report; besides automatism is not available for a hexa grid (due to a missing license for Autohexa) but is included into the tetra grid meshing procedure. Other automatism during the hexa meshing procedure can not be used due to problems with the flipper’s geometry file in terms of wholes and format. As it was complex associating blocking to the surface without tubercles, an exemplary mesh generation for a fin with tubercles is not possible. The surface in this case is a lot more complex and requires even more points to be set onto the surface, exponentiating the effort for meshing with hexa.

Consequently, as a recommendation for further research on this topic, the digitalized pectoral fin with and without tubercles should be meshed with a tetra mesh, using the automatism provided. Numerical analysis should prove or disprove the outcomes of the previously described panel method in chapter 3.2. The Reynolds Number must be adjusted, first according to the actual environment of the whale (chapter 2.2.1), then to the environment of the system where this improvement will be used later on (air, speed, characteristic length). Through literature research of the diving and swimming behavior, dimensionless numbers for dynamic similitude have to be determined. Key figures for calculating these numbers can also be found in chapter 2.2.1. Foraging velocity can be set up to 2.0 – 2.5 m/s, dive depth to 30 m [19]. For this simulation, the flipper is attacked at 120°-150° in the longitudinal axis, and 30°-40° in the downward angle, as seen in the according subchapter.

However, the panel method done in other research displays that solving a similar numerical problem is possible. Meshing a pectoral fin with a hexa mesh was the wrong approach. Setting up the mesh with tetrahedron meshes is recommended. Within Ansys ICEM CFD, automatism can create a tetra mesh efficiently. Figure 6-1 visualizes that hexa meshing was an inappropriate choice (left hand side), whereas tetra meshing might lead to a successful flow simulation.

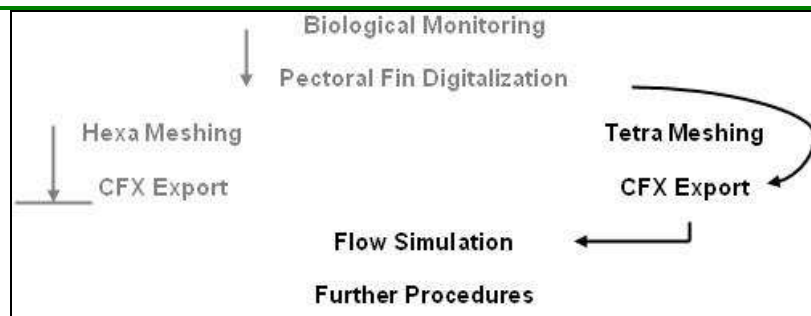


Figure 6-1: Flowchart of further recommendations on this topic



7 References

- [1] 7 SEAS WHALE WATCH, 7 Seas Wharf on Route 127, Gloucester, MA 01930
 - [2] Helen Heap, Bill Crowther , A Review of Current Leading Edge Device Technology and of Options for Innovation Based on Flow Control, University of Manchester, UK, June 2003
 - [3] ANSYS ICEM CFD/Al*Environment 10.0 User Manual
 - [4] ANSYS, Inc., Southpoint, 275 Technology Drive, Canonsburg, PA 15317
 - [5] Dolphin WF, Foraging dive patterns of humpback whales in southeast Alaska, Canadian Journal of Zoology 66, 1987
 - [6] <http://savci.upol.cz>, Copyright 2002-2005, List of Authors and Contributors on Webpage
 - [7] Chris Brady, <http://www.b737.org.uk>, 1999
 - [8] Wikimedia Foundation Inc., St. Petersburg, USA, <http://www.wikipedia.de>, 31st January,2007
 - [9] F. Fish, J.M. Battle, Hydrodynamic Design of the Humpback Whale Flipper, Journal of Morphology, 1995
 - [10] Ingo Rechenberg, Bionics & Evolution Technique, Technical University Berlin
 - [11] Dipl. Ing. Jens Andreas, CEO PicoLAS GmbH, kkonvert.c , Research associate at ISEA since January 2005
 - [12] Gerry Soejatman, JetPhotos.net, 31st January,2007
 - [13] John Gibbins, Union-Tribune, SignOnSanDiego.com, 31st January,2007
 - [14] D.S. Miklosovic, M.m. Murray, L.E. Howle, F.E. Fish, Leading-edge Tubercles delay stall on Humpback Whale (Megaptera Novaeangliae) flippers, 2003/2004
 - [15] Manuela Kirsch, FunActiv.de, Ludwigshafen / Bodensee
 - [16] Michael Stache, Bionics & Evolution Technique, Technical University Berlin
 - [17] Micro AeroDynamics Inc., 4000 Airport Road Suite "D", Anacortes WA 98221
 - [18] OAR/NURP/University of North Carolina at Wilmington, Netzeitung.de, 31st January, 2007
-



-
- [19] Springer Berlin / Heidelberg, Observations on Underwater Locomotion and Flipper Movement of the Humpback Whale, Marine Biology 48, 1978
 - [20] Kevin Chu, Sharon Nieukirk, Dorsal fin scars as indicators of age, sex, and soivial status in humpback whales (*Megaptera novaeangliae*), May 15, 1987
 - [21] presstext Nachrichtenagentur GmbH, article in "DerStandard.at", Wien, Austria, 31st January, 2007
 - [22] Provincetown Center for Coastal Studies, Provincetown, Massachusetts 02657, USA
 - [23] P. Watts, F.E. Fish, The Influence of Passive, Leading Edge Tubercles on Wing Performance, 12th Int. Symp. Unmanned Untethered Submesible Technology, Autonomous Undersea Systems Inst. Durham, NH, 2001
 - [24] Department for Mathematics, Philipps-Universität Marburg, consortium for data bionics, 2004
 - [25] Elisabeth Lemke, Jean C. Roché, *Wale, Giganten der Meere* (DE), 2002
 - [26] Winn, L.K. / Winn, H.E., *Wings in the Sea – The Humpback Whale*, 1985
 - [27] Variable camber leading edge mechanism with Krueger flap, United States Patent 4427168
 - [28] Uko Gorter Illustrations, AMERICAN CETACEAN SOCIETY, *Humpback Whale Skeleton*, 2004
 - [29] US Navy, Naval Postgraduate School, Department of Aeronautics and Astronautics, Online Tools, January 30th, 2007
-



8 Appendix

8.1 The “kkonvert.c” BMP-to-Coordinate Converter

8.1.1 Program Code

```
/*
BMP-to-Coordinates Converter:
*/

#include<stdio.h>
#include<stdlib.h>

short int bmp1ddat[1500000],
        bmp2ddat[1500,1000];
int    kfeld_x[1000],
        kfeld_y[1000],
        k_max,
        x_max,
        y_max,
        nachbar_x[2],
        nachbar_y[2];
const int offset_bmpxsize = 19;
const int offset_bmpysize = 23;
const int offset_bmpdata = 55;

FILE* bmpdat;
FILE* outdat;
FILE* felddat;

void readbmpsize (void);
void readbmpdata (void);
void convert_1d_to_2d (void);
void analyze_data (void);
    int anz_nachbarn (int xpos, int ypos);
void allocate_kfeld (void);
    void search3x3(int k);
    int num_new_point(int k);
void write_kfeld (void);
void closedata (void);

/*****
*****/
int main (int argc, char* argv[])
{
/*
if (argc = 1)
{
    printf("Mistake\n");
    exit;
}
*/
bmpdat = fopen("test.bmp", "r");
```



```

outdat = fopen("output.txt", "w");
felddat = fopen("2d_field.txt", "w");
readbmpsize();
readbmpdata();
convert_1d_to_2d();
analyze_data();
allocate_kfeld();
write_kfeld();
closedata();
return (0);
}

/*****
*****/
void readbmpsize (void)
/*Read BMP size from header. (return: zeilen(y_max), spalten(x_max))*/
{
int i;
unsigned char dummy,x1,x2,y1,y2;
for (i=1;i<offset_bmpxsize;i++)
    fscanf(bmpdat, "%c", &dummy);
fscanf(bmpdat, "%c", &x1);
fscanf(bmpdat, "%c", &x2);
x_max=x2*256+x1;
for (i=offset_bmpxsize+2;i<offset_bmpysize;i++)
    fscanf(bmpdat, "%c", &dummy);
fscanf(bmpdat, "%c", &y1);
fscanf(bmpdat, "%c", &y2);
y_max=y2*256+y1;
//printf("test %x %x %i\n",x1,x2,x_max);
//printf("test %x %x %i\n",y1,y2,y_max);
}

/*****
*****/
void readbmpdata (void)
/* read BMP data into 1d-Bool-Field.*/
/*(return: 1D-Bool-Feld)*/
{
int i,cnt,length;
unsigned char dummy;
/*positionieren am Anfang der Daten*/
for (i=offset_bmpysize+2;i<offset_bmpdata;i++)
    fscanf(bmpdat, "%c", &dummy);

/*calculate length of data set and save.*/
cnt=0;
length=x_max*y_max*3;
if (x_max!=y_max)
    length=length+y_max*2; //Special signatures in non square bmps.
//printf("read %i %i %i\n",length,x_max,y_max);
for (i=1;i<=length;i++)
{
    fscanf(bmpdat, "%c", &dummy);
    if (i%3 == 1)
    {
        cnt++;
        bmp1ddat[cnt]=0;
        if (dummy==00)

```



```
        {
            //printf("cnt ");
            bmp1ddat[cnt]=1;
        }
    }
}
}
/*****
*****/
void convert_1d_to_2d (void)
/*Convert 1d-Bool-Field into 2D-Bool-Field*/
/*Counts total dots in fin surface. */
{
int x,y,cnt;
k_max = 0;
cnt = 0;
for (y=1;y<=y_max;y++) {
    for (x=1;x<=x_max;x++) {
        cnt++;
        bmp2ddat[x,y]=bmp1ddat[cnt];
        if (bmp2ddat[x,y] == 1) /*actual dot is black.*/
        {
            if (x==1)
            {
                cnt++;
                bmp2ddat[x,y] = 0;
//                printf("%i,%i: %i\n",x,y,bmp2ddat[x,y]);
            }
            else
            {
                k_max++;
                fprintf(outdat, "%i,%i;",x,y);
            }
        }
//        fprintf(felddat, "%i",bmp2ddat[x,y]);
    }
//    fprintf(felddat, "\n");
}
//printf("found black dots: %i out of %i \n",k_max, cnt);
}

/*****
*****/
void analyze_data (void)
/*checking the three-times-three pixel square criteria*/
{
int anf_found = 0,
    end_found = 0,
    xpos,ypos;

for (ypos=2;ypos<y_max;ypos++) {
    for (xpos=2;xpos<x_max;xpos++) {
        if (bmp2ddat[xpos,ypos] == 1) /*actual dot is black*/
        {
            printf("%i,%i;",xpos,ypos);
            if (anz_nachbarn(xpos,ypos) == 1)
            {
                if (end_found == 1)
                {
                    printf("Fehler: More than 2 3x3-Squares\n");
                }
            }
        }
    }
}
}
```



```

        exit;
    }
    if (anf_found == 0) /*This point is start.*/
    {
        kfeld_x[1]=xpos;
        kfeld_y[1]=ypos;
        anf_found = 1;
    }
    if (anf_found == 1) /*This point is therefore end.*/
    {
        kfeld_x[k_max]=xpos;
        kfeld_y[k_max]=ypos;
        end_found = 1;
    }
}
if (anz_nachbarn(xpos,ypos) == 2)
    printf("Logically: Found 2 neighbors at x=%i,
y=%i.\n",xpos,ypos);
    if (anz_nachbarn(xpos,ypos) > 2)
        printf("Fehler: More than three dots in 3x3-square at x=%i
and y=%i\n",xpos,ypos);
    }
    fprintf(felddat, "%i",bmp2ddat[xpos,ypos]);
}
fprintf(felddat, "\n");
}
if (end_found == 0)
    printf("Error: 2 3x3-Squares with only 2 dots not found.\n");
if (end_found == 0 & anf_found == 0)
    printf("Error: No 3x3-Squares with only 2 dots found.\n");
}

int anz_nachbarn (int xpos, int ypos)
/*calculates amount of black dots around 3x3-square.*/
{
int x,y,sum;
sum=-1;
printf("test");
for (x=xpos-1;x<=xpos+1;x++) {
    for (y=ypos-1;y<=ypos+1;y++) {
        sum=sum+bmp2ddat[x,y];
    }
}
if (sum == -1)
    printf("sum ist %i\n",sum);
//if (cnt!=9)
//    printf("Error in subroutine: Not equal to 9 iterations.");
return (sum);
}

/*****
*****/
void allocate_kfeld (void)
{
int k_cnt, new_point;

search3x3(1);
kfeld_x[2]=nachbar_x[1];
kfeld_y[2]=nachbar_y[1];

```



```
for (k_cnt=2;k_cnt<k_max;k_cnt++)
{
    search3x3(k_cnt);
    new_point=num_new_point(k_cnt);
    kfeld_x[k_cnt+1]=nachbar_x[new_point];
    kfeld_y[k_cnt+1]=nachbar_y[new_point];
}
}

void search3x3(int k)
/*Finding x,y coordinates of neighbor dots of 3x3-square.*/
{
    int x,y,anz;
    anz=1;
    for (x=kfeld_x[22]-1;x<=kfeld_x[22]+1;x++) {
        for (y=kfeld_y[22]-1;y<=kfeld_y[22]+1;y++) {
            if (bmp2ddat[x,y] == 1) /*actual dot is black*/
            {
                nachbar_x[anz]=x;
                nachbar_y[anz]=y;
                anz++;
            }
        }
    }
}

int num_new_point(int k)
/*considers which neighbor dot is the "new" or the "old" one.*/
{
    if (kfeld_x[k-1]==nachbar_x[1] && kfeld_y[k-1]==nachbar_y[1])
        return 2;
    return 1;
}

/*****
*****/
void write_kfeld (void)
/*writes k-field in output file.*/
{
    int i;
    for (i=1;i<=k_max;i++)
        printf("%i \t%i\n",kfeld_x[i],kfeld_y[i]);
}

/*****
*****/
void closedata (void)
{
    fclose(bmpdat);
    fclose(outdat);
    fclose(felddat);
}
```



8.2 CD Index

- Appendix
 - Kkonvert.c
 - Profil mit Tuberkeln – Koordinaten.txt
 - Profil ohne Tuberkel – Koordinaten.txt
- Excel
 - Auszug aus TecPlot.xls
 - Distribution Dives.xls
 - Echo_Sounder.xls
 - Feldpunkte_kurz_mit_Tuberkel.xls
 - Feldpunkte_kurz_ohne_Tuberkel.xls
 - Flossen_skaliert.xls
 - Flossenprofil mit Tuberkel.xls
 - Liste Profilschnitte.xls
 - OptiProcess.xls
 - Profil mit Tuberkel Schnitte.xls
 - References.xls
- Images
 - Flipper Drawings
 - Screenshots ProE
 - Other Screenshots
 - Various Images
- Papers
 - Hydrodynamic Design of the Humpback Whale Flipper.pdf
- Whale Song
 - Whale Song.mp3
 - Whale Song.ogg
- Report
 - Report_IST.pdf



8.3 Additional Tables

Y	X1	Chord	X2
1	0,085789	0,014731	0,071058
0,996534	0,097054	0,033795	0,063259
0,948873	0,146447	0,083189	0,063258
0,889948	0,175043	0,10052	0,074523
0,831023	0,191508	0,109185	0,082323
0,772097	0,20364	0,124783	0,078857
0,713172	0,214905	0,143847	0,071058
0,654246	0,222704	0,159445	0,063259
0,595321	0,227903	0,17331	0,054593
0,536395	0,229636	0,187175	0,042461
0,47747	0,230503	0,200173	0,03033
0,418544	0,228769	0,210572	0,018197
0,359619	0,227036	0,219237	0,007799
0,300693	0,22617	0,225303	0,000867
0,241768	0,22357	0,216638	0,006932
0,182842	0,214905	0,190641	0,024264
0,123917	0,205373	0,168111	0,037262
0,064991	0,20364	0,158579	0,045061
0,006066	0,202773	0,159445	0,043328

Table 8-1: List of Coordinates for Pectoral Fin without Tubercles



Y	X1	Chord	X2
0,999114	0,085993	0,012411	0,073582
0,998227	0,10727	0,02305	0,08422
0,995567	0,114362	0,047872	0,06649
0,992908	0,119681	0,059397	0,060284
0,968085	0,132092	0,072695	0,059397
0,952128	0,156028	0,093085	0,062943
0,925532	0,162234	0,091312	0,070922
0,901596	0,179965	0,110816	0,069149
0,875886	0,187057	0,106383	0,080674
0,849291	0,18883	0,10461	0,08422
0,822695	0,20922	0,125	0,08422
0,796099	0,203014	0,12234	0,080674
0,77039	0,219858	0,140957	0,078901
0,743794	0,218972	0,143617	0,075355
0,717199	0,210993	0,139184	0,071809
0,691489	0,231383	0,164007	0,067376
0,664894	0,233156	0,169326	0,06383
0,638298	0,221631	0,162234	0,059397
0,611702	0,223404	0,170213	0,053191
0,585993	0,249113	0,202128	0,046985
0,559397	0,250887	0,208333	0,042554
0,532801	0,234043	0,195035	0,039008
0,506206	0,242021	0,208333	0,033688
0,47961	0,23227	0,204787	0,027483
0,453014	0,242908	0,221631	0,021277
0,426418	0,241135	0,226064	0,015071
0,399823	0,230496	0,220745	0,009751
0,373227	0,238475	0,231383	0,007092
0,346631	0,243794	0,240248	0,003546
0,320035	0,22961	0,228723	0,000887
0,29344	0,225177	0,225177	0
0,266844	0,234043	0,23227	0,001773
0,240248	0,25	0,244681	0,005319
0,213652	0,237589	0,22695	0,010639
0,187057	0,217199	0,199468	0,017731
0,160461	0,20922	0,184397	0,024823
0,133865	0,207447	0,176418	0,031029
0,10727	0,204787	0,16844	0,036347
0,083333	0,203014	0,163121	0,039893
0,056738	0,202128	0,160461	0,041667
0,030142	0,200355	0,157801	0,042554
0,003546	0,201241	0,158688	0,042553

Table 8-2: List of Coordinates for Pectoral Fin with Tubercles



[mm]	ProE z	ProE x	ProE y	
Section	Y-coordinate	Length	Starting point	
	0,0000	Z	X	
1	10,6380	10,6380	0,5998	625,0020
2	90,4260	79,7880	0,5965	624,9990
3	170,2140	79,7880	0,6065	627,6600
4	249,9990	79,7850	0,6166	632,9820
5	321,8100	71,8110	0,6367	643,6200
6	401,5950	79,7850	0,6669	659,5740
7	481,3830	79,7880	0,6970	678,1920
8	561,1710	79,7880	0,7540	699,4680
9	640,9560	79,7850	0,8579	720,7440
10	720,7440	79,7880	0,9249	736,7040
11	800,5320	79,7880	0,8780	747,3420
12	880,3200	79,7880	0,8512	752,6610
13	960,1050	79,7850	0,8646	750,0000
14	1039,8930	79,7880	0,9081	742,0230
15	1119,6810	79,7880	0,8746	731,3850
16	1199,4690	79,7880	0,8344	723,4080
17	1279,2540	79,7850	0,8545	707,4480
18	1359,0420	79,7880	0,8378	688,8300
19	1438,8300	79,7880	0,7741	670,2120
20	1518,6179	79,7879	0,7875	651,5970
21	1598,4029	79,7850	0,7372	635,6370
22	1678,1909	79,7880	0,7875	624,9990
23	1757,9790	79,7881	0,7640	611,7060
24	1835,1061	77,1271	0,6434	593,0880
25	1914,8939	79,7878	0,6132	574,4700
26	1994,6820	79,7881	0,6401	561,1710
27	2074,4669	79,7849	0,6199	550,5330
28	2151,5971	77,1302	0,5261	537,2340
29	2231,3821	79,7850	0,5429	526,5960
30	2311,1699	79,7878	0,5328	515,9580
31	2388,2970	77,1271	0,4624	510,6390
32	2468,0851	79,7881	0,4725	500,0010
33	2547,8731	79,7880	0,3954	500,0010
34	2627,6581	79,7850	0,4021	510,6390
35	2704,7880	77,1299	0,4189	545,2140
36	2776,5960	71,8080	0,3452	539,8950
37	2856,3840	79,7880	0,3519	563,8320
38	2904,2550	47,8710	0,2748	574,4700
39	2978,7240	74,4690	0,2245	571,8090
40	2986,7011	7,9771	0,1810	553,1910
41	2994,6810	7,9799	0,0871	500,0010
42	2997,3419	2,6609	0,4690	531,9150

Table 8-3: Airfoil Cuts for Pectoral Fin with Tubercles



German	English
Auge	eye
Blaslöcher	blow holes
Brustflosse	pectoral fin / flipper
Kehlfurchen	throat furrows
mittlere Kerbe	middle notch
Oberkiefer	upper jaw
Ohr	ear
Rückenflosse (Finne)	dorsal fin
Schwanzflosse	caudal fin / fluke
Schwanzstiel	tail shaft
Unterkiefer	lower jaw

Table 8-4: Translations

8.4 About the Author

Individual Facts

Home address: 28 Altenhellefelder Str,
D-59846 Sundern, Germany

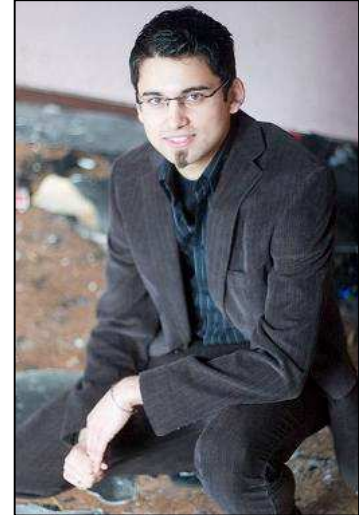
Telephone: (+49) 177 347 10 52

Email: carsten.wortmann@rwth-aachen.de

Date of Birth: Mai 29th, 1981

Place of Birth: Arnsberg, Germany

Nationality: German



Education

04/01 Enrolled at RWTH Aachen University of Technology, Germany

04/01 – 09/01 Preterm in Physics und Mathematics

Since 09/01 Studies of Aeronautics and Aerospace Engineering
Modules: Aerodynamics, Aircraft Design, Aeronautical Engines

04/06 – 08/06 Royal Melbourne Institute of Technology (RMIT), Australia

Research Projects

04/06 – 08/06 Research Project: "Preliminary Design of a Multi-Mission Unmanned Aerial Vehicle", RMIT Melbourne, Australia

08/05 – 12/06 Research Project: „Num. simulation of a humpback whale’s fin“
Institute of Jet Propulsion and Turbomachinery, RWTH Aachen

Engineering Internships

02/05 – 07/05 Trainee Engineering F.A.L. Support, **Airbus Toulouse**, France
Quality Assurance and Process Control

09/02 – 10/02 Trainee at **Air Berlin**, Airport Berlin-Tegel and Paderborn-Lippstadt
Resource Scheduling and Maintenance

[Referee’s details are available on request]